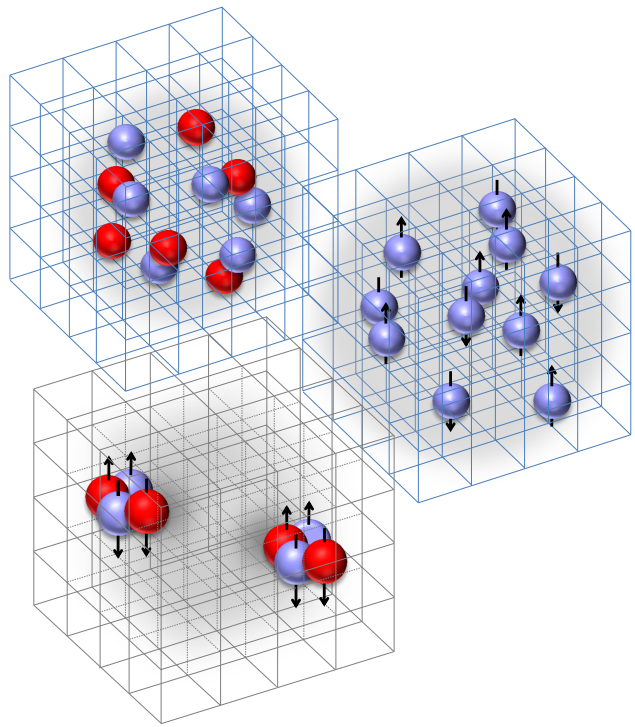
Ab Initio nuclear scattering and reactions with high-fidelity chiral interactions on the lattice

Serdar Elhatisari

Gaziantep Islam Science and Technology University, Gaziantep

Workshop on Few-Body Problems
in Nuclear and Hadron Physics
Institute of Theoretical Physics (ITP)
Chinese Academy of Sciences
September 21-24, 2026 , Beijing, China



When do we really need *ab initio* reactions?

Predictive reaction theory beyond the region directly constrained by data.

Nunes *et al.*, *Annu. Rev. Nucl. Part. Sci.* 70, 147 (2020)
Bernstein *et al.*, *Annu. Rev. Nucl. Part. Sci.* 69, 109 (2019)
Hebborn *et al.*, *J. Phys. G 50*, 060501 (2023).

- **Energies we cannot reach**
  - Stellar energies can lie far below the Coulomb barrier:
    $\Rightarrow$ Direct cross sections may become too small to measure.
- **Nuclei we cannot target**
  - Short-lived nuclei cannot always be prepared as targets:
    $\Rightarrow$ Neutron-induced reactions have no conventional free-neutron target for inverse kinematics.
- **Reaction space we cannot map**
  - Astrophysics and nuclear-data applications require many isotopes, energies, and channels:
    $\Rightarrow$ Experiment cannot map them all.

When do we really need *ab initio* reactions?

Predictive reaction theory beyond the region directly constrained by data.

Nunes *et al.*, *Annu. Rev. Nucl. Part. Sci.* 70, 147 (2020)
Bernstein *et al.*, *Annu. Rev. Nucl. Part. Sci.* 69, 109 (2019)
Hebborn *et al.*, *J. Phys. G 50*, 060501 (2023).

- **Energies we cannot reach**
  - Stellar energies can lie far below the Coulomb barrier:
    $\Rightarrow$ Direct cross sections may become too small to measure.
- **Nuclei we cannot target**
  - Short-lived nuclei cannot always be prepared as targets:
    $\Rightarrow$ Neutron-induced reactions have no conventional free-neutron target for inverse kinematics.
- **Reaction space we cannot map**
  - Astrophysics and nuclear-data applications require many isotopes, energies, and channels:
    $\Rightarrow$ Experiment cannot map them all.

When do we really need *ab initio* reactions?

Predictive reaction theory beyond the region directly constrained by data.

Nunes *et al.*, *Annu. Rev. Nucl. Part. Sci.* 70, 147 (2020)
Bernstein *et al.*, *Annu. Rev. Nucl. Part. Sci.* 69, 109 (2019)
Hebborn *et al.*, *J. Phys. G 50*, 060501 (2023).

- **Energies we cannot reach**
  - Stellar energies can lie far below the Coulomb barrier:
    $\Rightarrow$ Direct cross sections may become too small to measure.
- **Nuclei we cannot target**
  - Short-lived nuclei cannot always be prepared as targets:
    $\Rightarrow$ Neutron-induced reactions have no conventional free-neutron target for inverse kinematics.
- **Reaction space we cannot map**
  - Astrophysics and nuclear-data applications require many isotopes, energies, and channels:
    $\Rightarrow$ Experiment cannot map them all.

When do we really need *ab initio* reactions?

Predictive reaction theory beyond the region directly constrained by data.

Nunes *et al.*, *Annu. Rev. Nucl. Part. Sci.* 70, 147 (2020)
Bernstein *et al.*, *Annu. Rev. Nucl. Part. Sci.* 69, 109 (2019)
Hebborn *et al.*, *J. Phys. G 50*, 060501 (2023).

- **Energies we cannot reach**
  - Stellar energies can lie far below the Coulomb barrier:
    $\Rightarrow$ Direct cross sections may become too small to measure.
- **Nuclei we cannot target**
  - Short-lived nuclei cannot always be prepared as targets:
    $\Rightarrow$ Neutron-induced reactions have no conventional free-neutron target for inverse kinematics.
- **Reaction space we cannot map**
  - Astrophysics and nuclear-data applications require many isotopes, energies, and channels:
    $\Rightarrow$ Experiment cannot map them all.

Why go beyond bound-state observables?

Has the Hamiltonian that reproduces nuclear structure been fully tested?

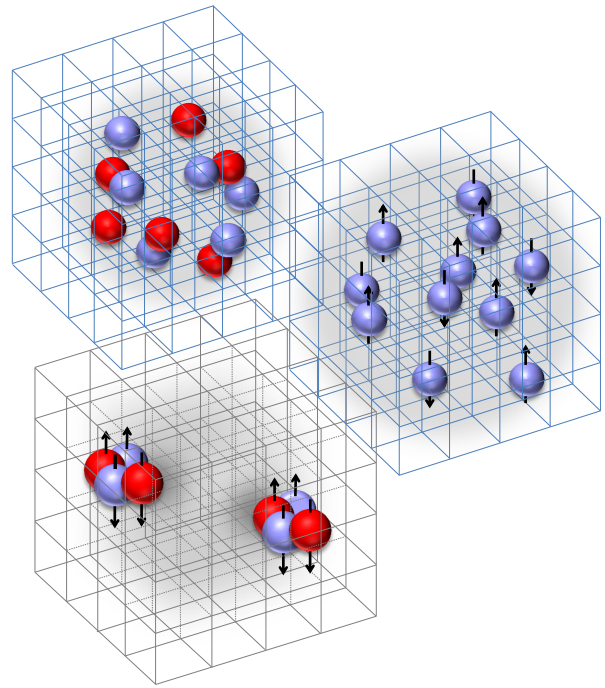
Bound states	$\Longleftrightarrow$	**Continuum**
☐ Energies, radii, spectra, electromagnetic observables.		☐ Phase shifts, resonances, cross sections and reaction amplitudes.
☐ Probe selected normalizable eigenstates of the Hamiltonian.		☐ Probe the Hamiltonian away from bound configurations.
☐ Strongly constrain the interaction around energetically favored configurations.		☐ Test whether thresholds, resonances and channel couplings emerge consistently.

Scattering and reactions provide an independent and often more stringent test of microscopic nuclear forces.

Johnson *et al.*, *J. Phys. G* 47, 123001 (2020)
Quaglioni *et al.*, *Nucl. Phys. A* 1060, 123095 (2025).

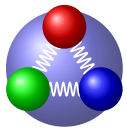
Outline

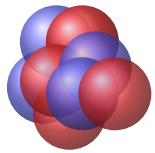
- Introduction
- Nuclear forces from QCD
- Effective field theories
- Lattice effective field theory
- Recent progress
- Scattering and reactions on the lattice
- Summary

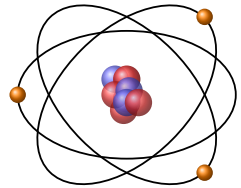


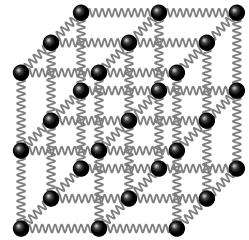
Why chiral EFT?


Quarks
$< 10^{-16}$

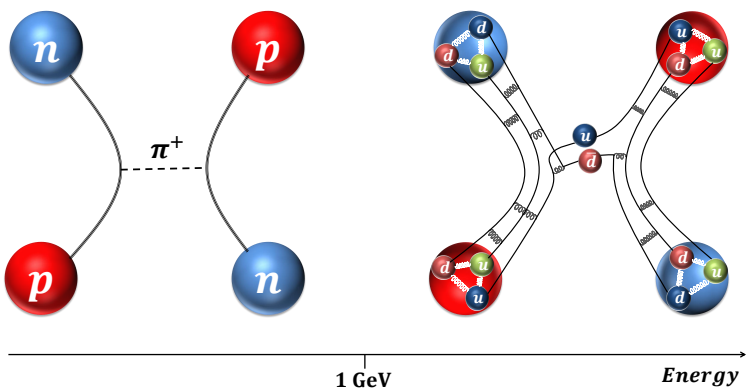

Nucleons
$\sim 10^{-13}$


Nucleus
$\sim 10^{-12}$


Atoms
$\sim 10^{-8}$ cm


Matter

- Quantum chromodynamics (QCD) describes the strong forces by confining quarks (and gluons) into baryons and mesons.
- At low energy: $N = (p, n)$, $\pi = (\pi^+, \pi^0, \pi^-)$
- Translating QCD directly into nuclear forces:



"separation of scales"

Λ_χ : chiral symmetry-breakdown scale

$m_u, m_d, m_s \to 0$ chiral limit

S. Weinberg, *Phys. Lett. B* 251 (1990) 288, *Nucl. Phys.* B363 (1991) 3, *Phys. Lett. B* 295 (1992) 114.

- Effective theories provide the solution to bridge the gap between QCD and the nuclear interactions

Chiral EFT for nucleons: nuclear forces

Chiral effective field theory organizes the nuclear interactions as an expansion in powers of momenta and other low energy scales such as the pion mass (Q/Λ_χ).

- Short distances are not resolved explicitly; they are encoded in contact operators.
- Long-range physics: pion exchange.
- Many-body physics: three- and higher-nucleon forces.

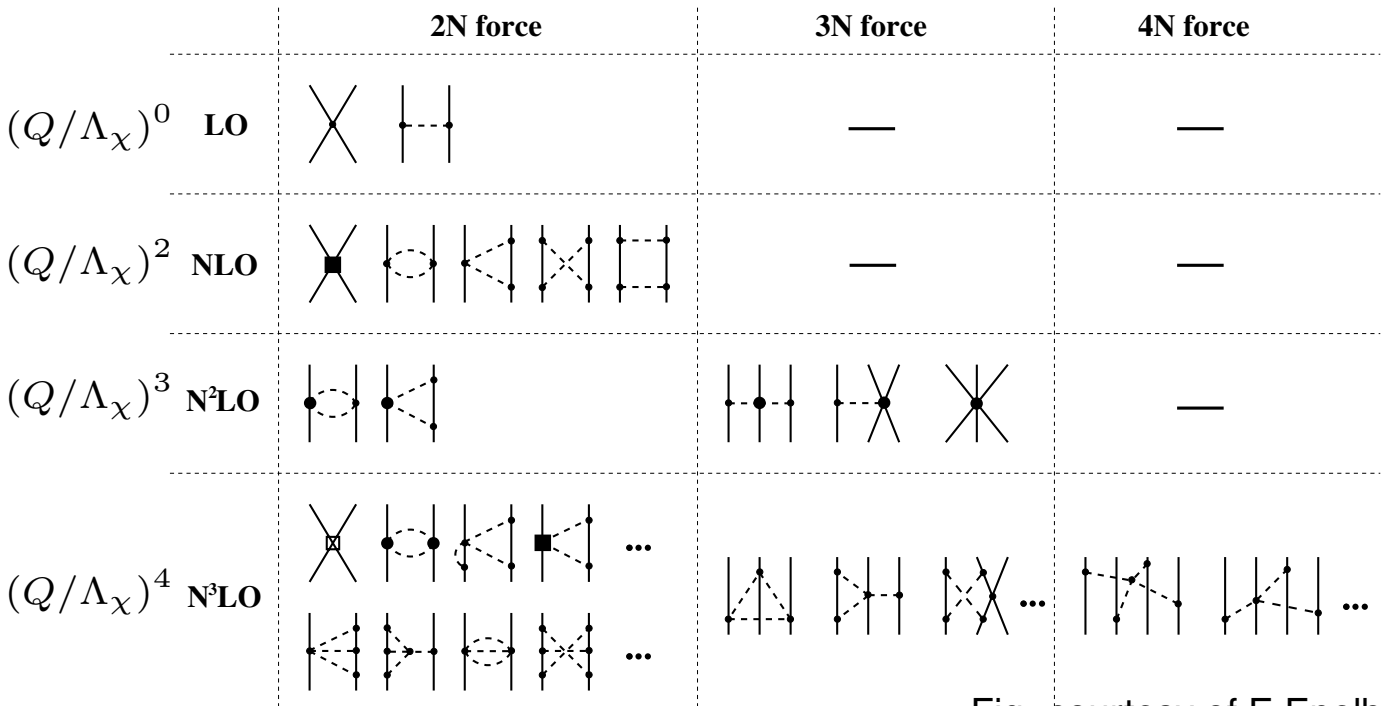
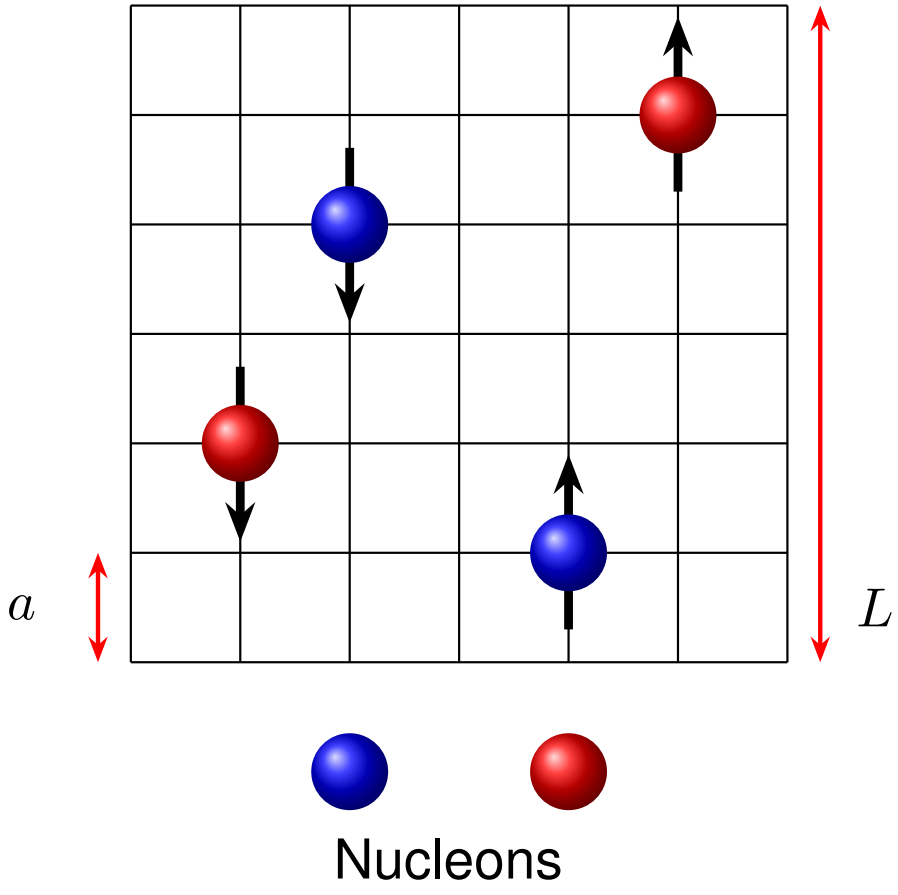


Fig. courtesy of E.Epelbaum

Ordonez et al. '94; Friar & Coon '94; Kaiser et al. '97; Epelbaum et al. '98,'03,'05,'15; Kaiser '99-'01; Higa et al. '03; ...

Lattice effective field theory: Why a lattice?

- Lattice effective field theory is a powerful numerical method formulated in the framework of chiral effective field theory.
- Lattice EFT is a regulated EFT, not merely a numerical grid method.



$\Rightarrow \quad \mathbf{x} = a\,\mathbf{n}, \quad \mathbf{n} = (n_x, n_y, n_z)$

$\Rightarrow \quad p_{\max} = \pi/a$

$\Rightarrow$ UV regulator: $\Lambda \sim \pi/a$

$\Rightarrow$ finite volume: $L_{phys} = L\,a$

$\Rightarrow$ finite-dimensional Hilbert space

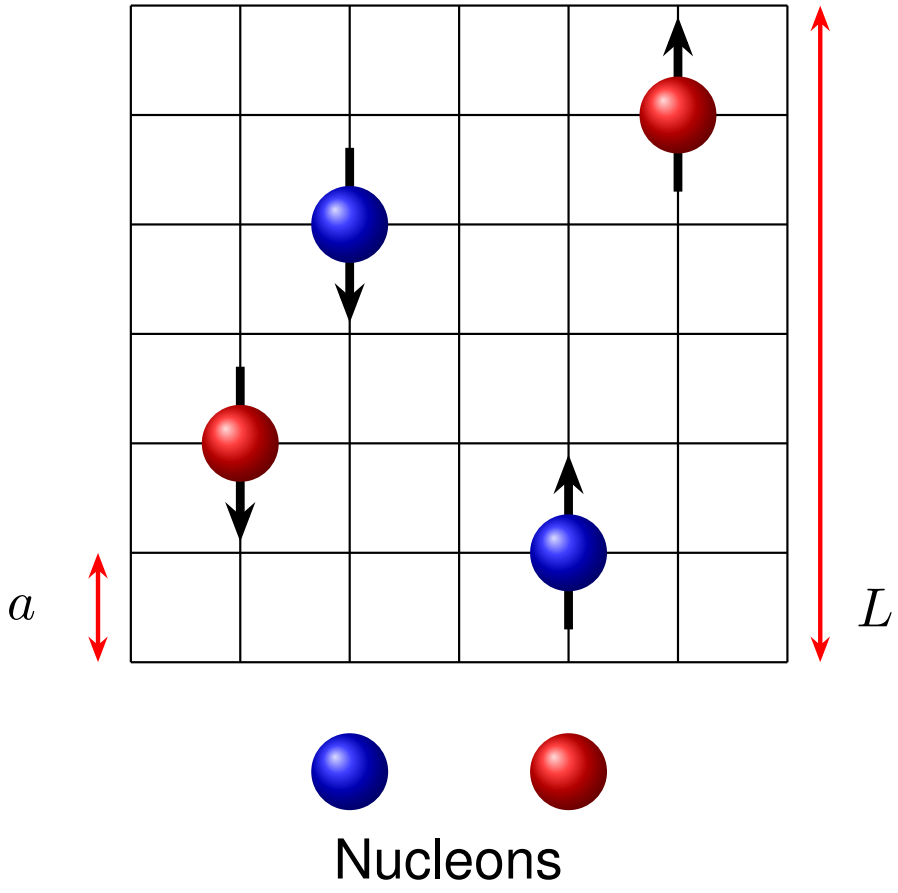
$\Rightarrow$ direct access to exact diagonalization and Monte Carlo

Lee, Prog.Part.Nucl.Phys. 63 (2009) 117-154

Laehde and Meißner, Lect. Notes Phys. 957 (2019), 1-396 Springer.

Lattice effective field theory: Why a lattice?

- Lattice effective field theory is a powerful numerical method formulated in the framework of chiral effective field theory.
- Lattice EFT is a regulated EFT, not merely a numerical grid method.



$\Rightarrow \quad \mathbf{x} = a\,\mathbf{n}, \quad \mathbf{n} = (n_x, n_y, n_z)$

$\Rightarrow \quad p_{\max} = \pi/a$

$\Rightarrow$ UV regulator: $\Lambda \sim \pi/a$

$\Rightarrow$ finite volume: $L_{phys} = L\,a$

$\Rightarrow$ finite-dimensional Hilbert space

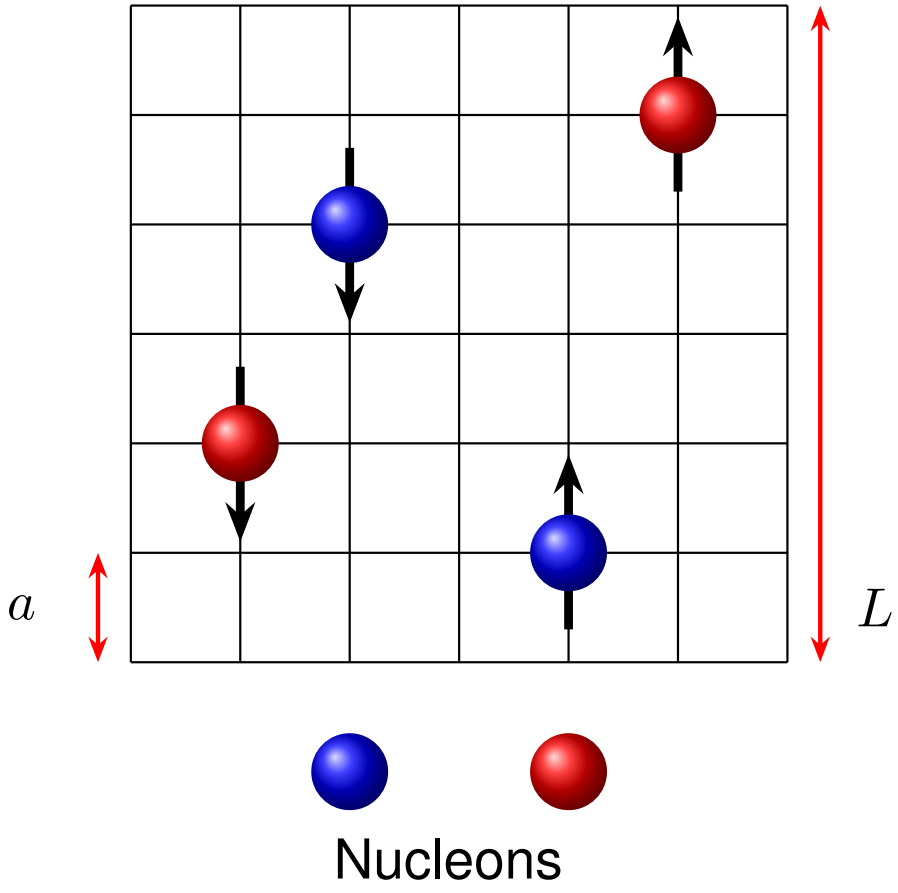
$\Rightarrow$ direct access to exact diagonalization and Monte Carlo

Lee, Prog.Part.Nucl.Phys. 63 (2009) 117-154

Laehde and Meißner, Lect. Notes Phys. 957 (2019), 1-396 Springer.

Lattice effective field theory: Why a lattice?

- Lattice effective field theory is a powerful numerical method formulated in the framework of chiral effective field theory.
- Lattice EFT is a regulated EFT, not merely a numerical grid method.



$\Rightarrow \quad \mathbf{x} = a\,\mathbf{n}, \quad \mathbf{n} = (n_x, n_y, n_z)$

$\Rightarrow \quad p_{\max} = \pi/a$

$\Rightarrow$ UV regulator: $\Lambda \sim \pi/a$

$\Rightarrow$ finite volume: $L_{phys} = L\,a$

$\Rightarrow$ finite-dimensional Hilbert space

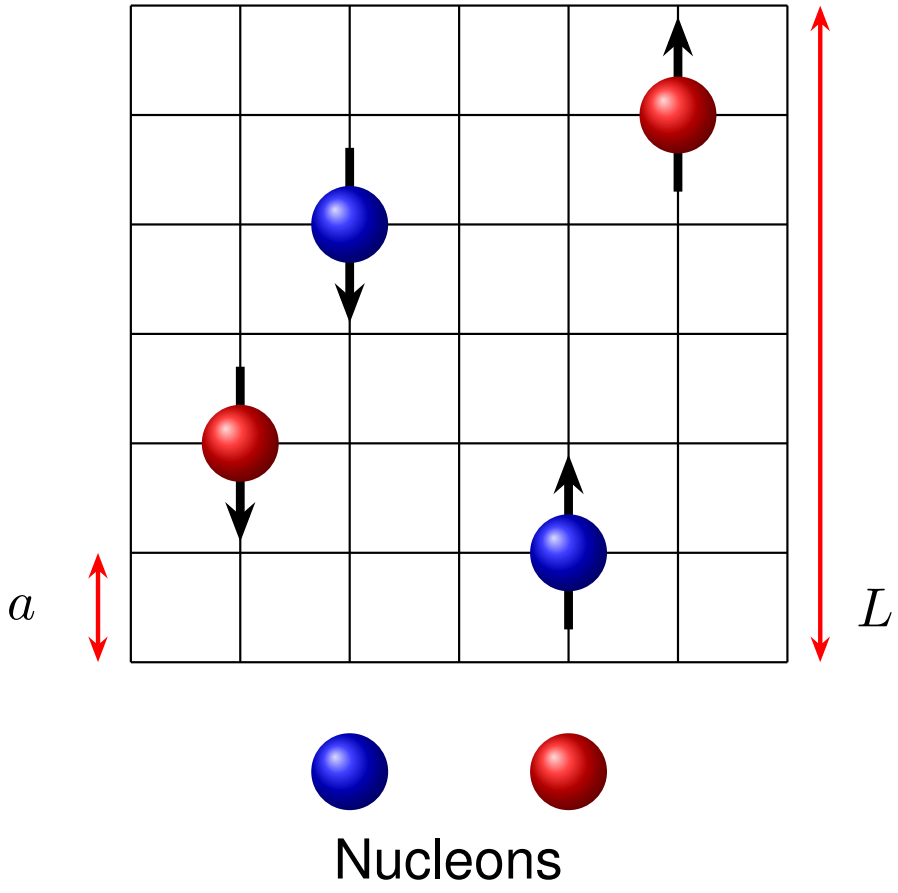
$\Rightarrow$ direct access to exact diagonalization and Monte Carlo

Lee, Prog.Part.Nucl.Phys. 63 (2009) 117-154

Laehde and Meißner, Lect. Notes Phys. 957 (2019), 1-396 Springer.

Lattice effective field theory: Why a lattice?

- Lattice effective field theory is a powerful numerical method formulated in the framework of chiral effective field theory.
- Lattice EFT is a regulated EFT, not merely a numerical grid method.



$\Rightarrow \quad \mathbf{x} = a\,\mathbf{n}, \quad \mathbf{n} = (n_x, n_y, n_z)$

$\Rightarrow \quad p_{\max} = \pi/a$

$\Rightarrow$ UV regulator: $\Lambda \sim \pi/a$

$\Rightarrow$ finite volume: $L_{phys} = L\,a$

$\Rightarrow$ finite-dimensional Hilbert space

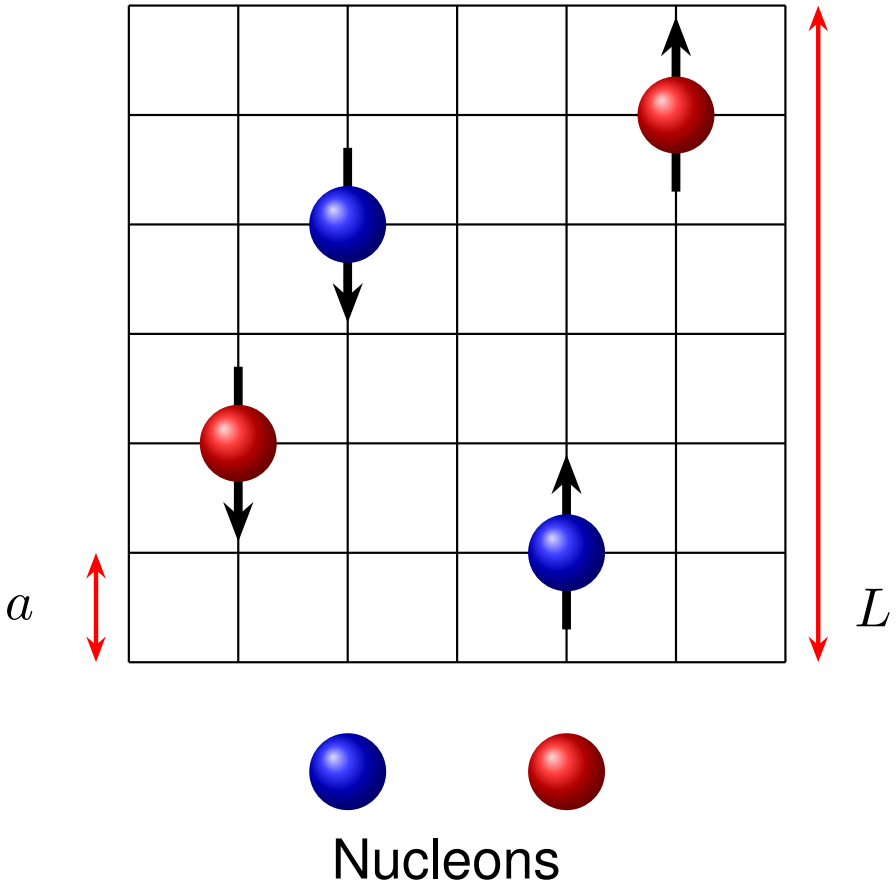
$\Rightarrow$ direct access to exact diagonalization and Monte Carlo

Lee, Prog.Part.Nucl.Phys. 63 (2009) 117-154

Laehde and Meißner, Lect. Notes Phys. 957 (2019), 1-396 Springer.

Lattice effective field theory: Why a lattice?

- Lattice effective field theory is a powerful numerical method formulated in the framework of chiral effective field theory.
- Lattice EFT is a regulated EFT, not merely a numerical grid method.



$\Rightarrow \quad \mathbf{x} = a\,\mathbf{n}, \quad \mathbf{n} = (n_x, n_y, n_z)$

$\Rightarrow \quad p_{\max} = \pi/a$

$\Rightarrow$ UV regulator: $\Lambda \sim \pi/a$

$\Rightarrow$ finite volume: $L_{phys} = L\,a$

$\Rightarrow$ finite-dimensional Hilbert space

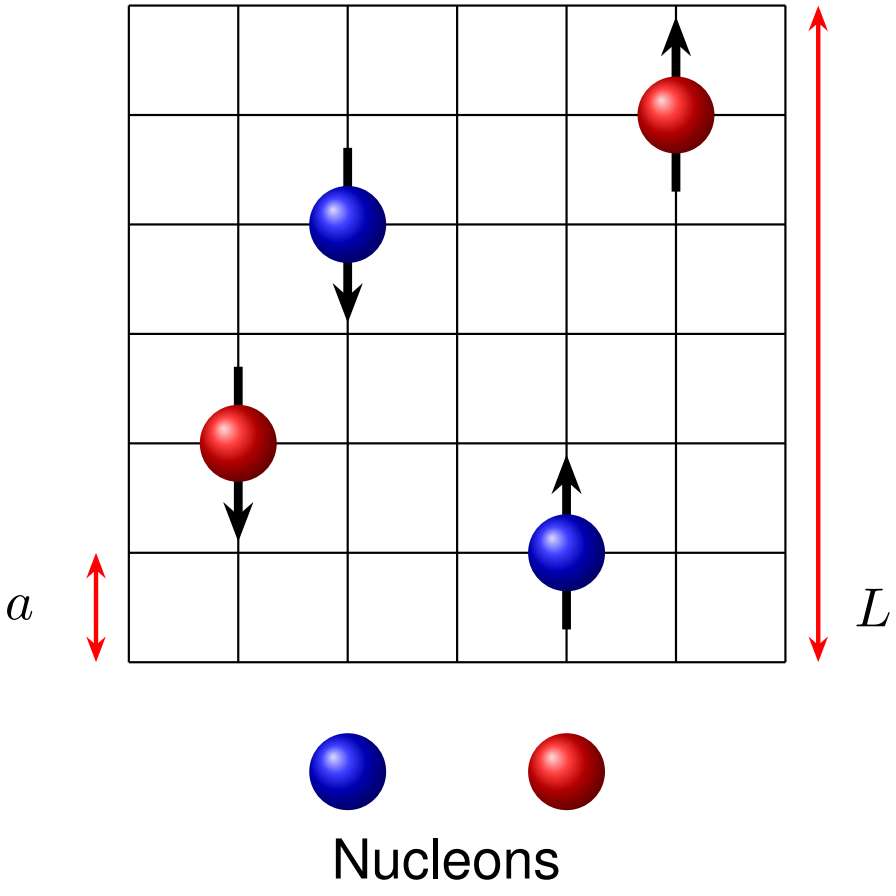
$\Rightarrow$ direct access to exact diagonalization and Monte Carlo

Lee, Prog.Part.Nucl.Phys. 63 (2009) 117-154

Laehde and Meißner, Lect. Notes Phys. 957 (2019), 1-396 Springer.

Lattice effective field theory: Why a lattice?

- Lattice effective field theory is a powerful numerical method formulated in the framework of chiral effective field theory.
- Lattice EFT is a regulated EFT, not merely a numerical grid method.



$\Rightarrow \quad \mathbf{x} = a\,\mathbf{n}, \quad \mathbf{n} = (n_x, n_y, n_z)$

$\Rightarrow \quad p_{\max} = \pi/a$

$\Rightarrow$ UV regulator: $\Lambda \sim \pi/a$

$\Rightarrow$ finite volume: $L_{phys} = L\,a$

$\Rightarrow$ finite-dimensional Hilbert space

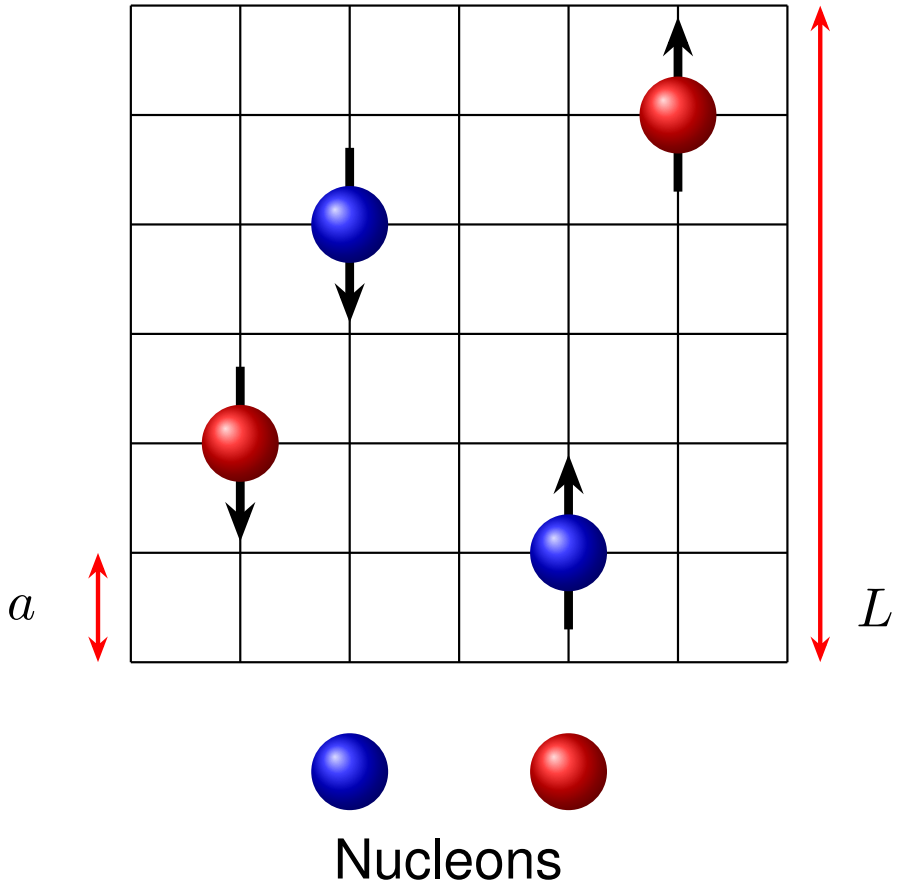
$\Rightarrow$ direct access to exact diagonalization and Monte Carlo

Lee, Prog.Part.Nucl.Phys. 63 (2009) 117-154

Laehde and Meißner, Lect. Notes Phys. 957 (2019), 1-396 Springer.

Lattice effective field theory: Why a lattice?

- Lattice effective field theory is a powerful numerical method formulated in the framework of chiral effective field theory.
- Lattice EFT is a regulated EFT, not merely a numerical grid method.



$\Rightarrow \quad \mathbf{x} = a\,\mathbf{n}, \quad \mathbf{n} = (n_x, n_y, n_z)$

$\Rightarrow \quad p_{\max} = \pi/a$

$\Rightarrow$ UV regulator: $\Lambda \sim \pi/a$

$\Rightarrow$ finite volume: $L_{phys} = L\,a$

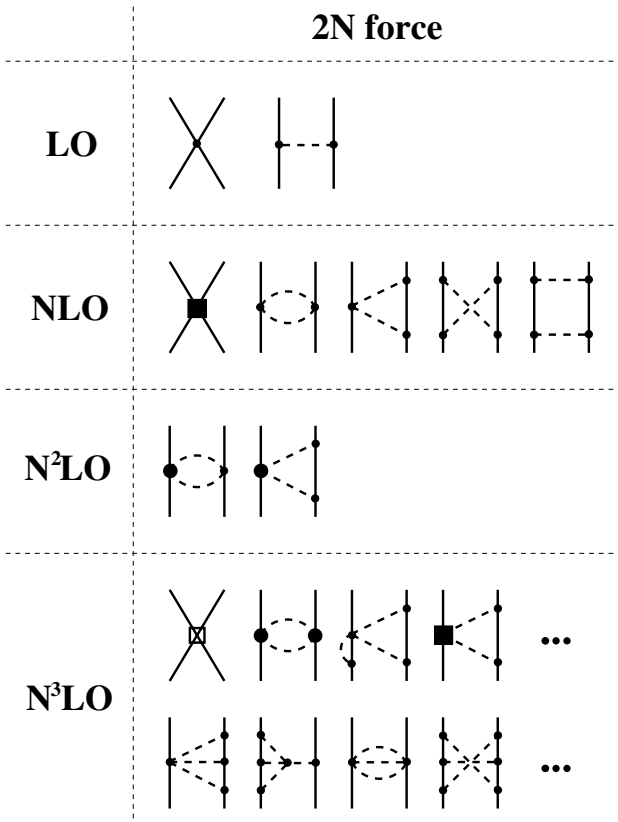
$\Rightarrow$ finite-dimensional Hilbert space

$\Rightarrow$ direct access to exact diagonalization and Monte Carlo

Lee, Prog.Part.Nucl.Phys. 63 (2009) 117-154

Laehde and Meißner, Lect. Notes Phys. 957 (2019), 1-396 Springer.

Chiral EFT for nucleons: *NN* scattering phase shifts

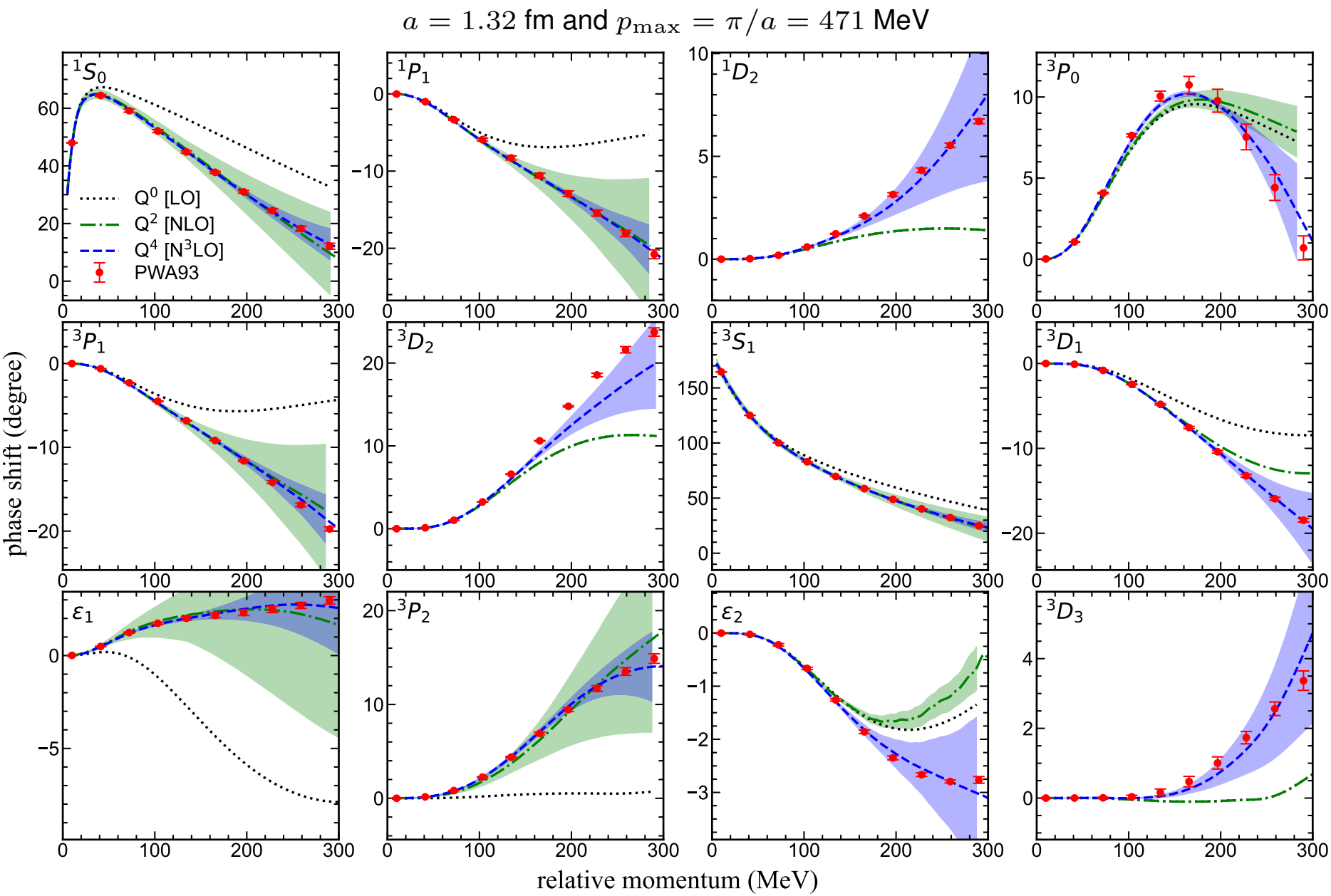


$\Longleftrightarrow$ $V_{0,^1S_0}$ $V_{0,^3S_1}$

$\Longleftrightarrow$ $V_{2,^1S_0}$ $V_{2,^3S_1}$ $V_{2,^3SD}$ $V_{2,^1P_1}$ $V_{2,^3P_0}$ $V_{2,^3P_1}$ $V_{2,^3P_2}$

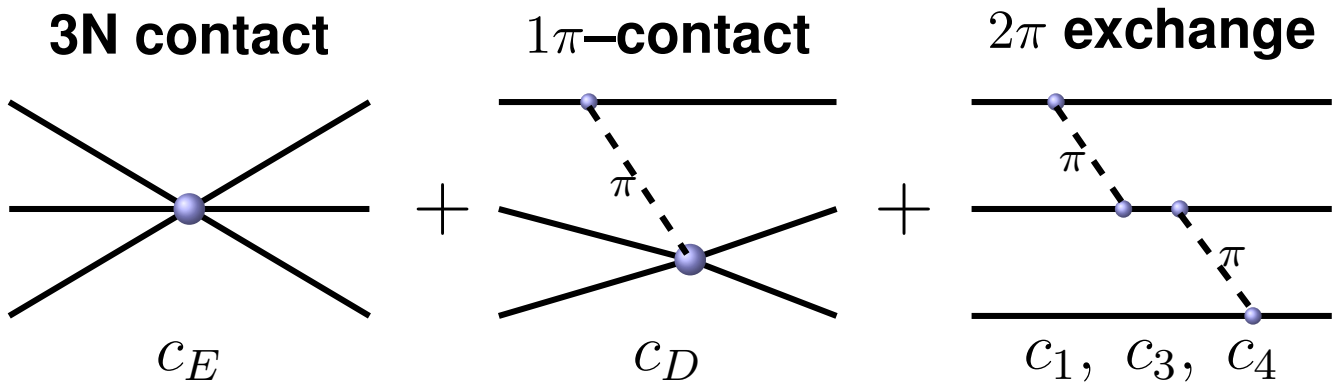
$\Big\}$ $V^{(1)}_{4,^1S_0}$ $V^{(2)}_{4,^1S_0}$ $V^{(1)}_{4,^3S_1}$ $V^{(2)}_{4,^3S_1}$ $V^{(1)}_{4,^3SD}$ $V^{(2)}_{4,^3SD}$ $V_{4,^1P_1}$ $V_{4,^3P_0}$ $V_{4,^3P_1}$ $V_{4,^3P_2}$ $V_{4,^3PF}$ $V_{4,^1D_2}$ $V_{4,^3D_1}$ $V_{4,^3D_2}$ $V_{4,^3D_3}$

Lattice formulation of chiral EFT



The leading three-nucleon force at N^{2}LO

$$V_{3N}^{(\mathrm{N^2LO})} = V_{2\pi}(c_1, c_3, c_4) + V_{1\pi\text{-ct}}(c_D) + V_{\mathrm{ct}}(c_E).$$



Already constrained

$c_1,\ c_3,\ c_4$

come from pion–nucleon and two-nucleon physics and also enter the long-range $3N$ force.

New 3N LECs

$c_D,\quad c_E$

must be constrained using observables in systems with $A \geq 3$.

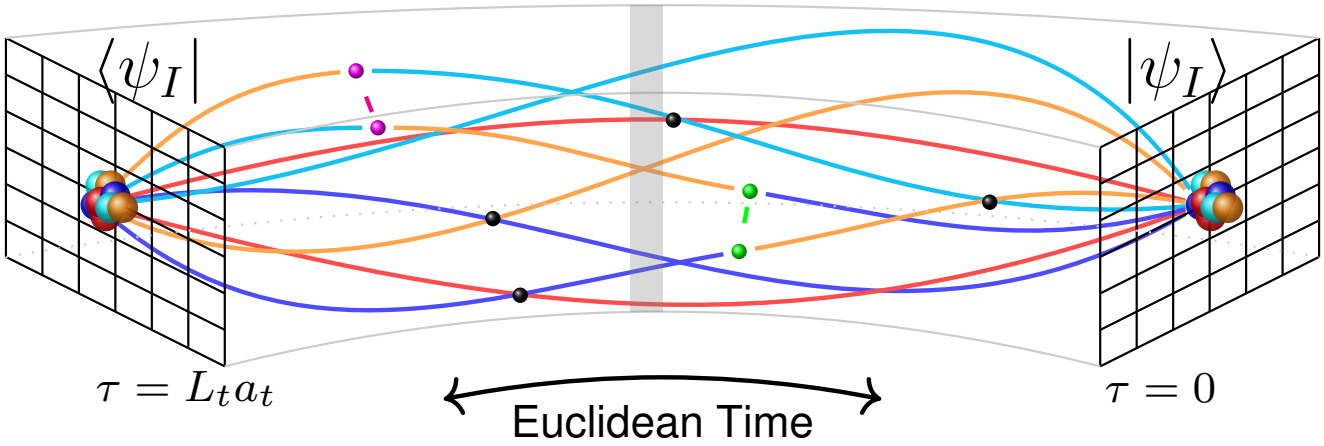
$$(c_D, c_E) \xrightarrow{\text{fit to independent few-body data}} E_{^3\mathrm{H}},\ a_{nd}^{(2)},\ M_{\mathrm{GT}},\ E_{^4\mathrm{He}},\ \ldots$$

Chiral EFT for nucleons: 3NFs

Work	Constraints	Predictions
NCSM, Barrett *et al.*, Nogga *et al.*	BE of ^{3}H and ^{4}He	Spectrum of ^{6}Li and ^{7}Li
NCSM, Navratil *et al.*	^{3}H, ^{6}Li, ^{10}B, ^{12}C	^{4}He, ^{6}Li, ^{10,11}B, ^{12,13}C
NCSM, Maris *et al.*, Roth *et al.*	BE of ^{3}H and ^{3}H β decay	Structures of $A = 7, 8$. ^{4}He, ^{6}Li, ^{12}C and ^{16}O
CC, Hagen *et al.*	BE of ^{3}H and ^{3}H β decay	EoS of nucleonic matter
BMBPT, Tichai *et al.*	BE of ^{3}H and ^{3}H β decay	BE of $^{16-26}$O, $^{36-60}$Ca and $^{50-78}$Ni
IT-NCSM, Roth *et al.*	BE of ^{3}H and ^{4}He, and ^{3}H β decay	BE of ^{4}He, ^{16}O, ^{40}Ca
CC, Roth *et al.*	BE of ^{3}H and ^{4}He, and ^{3}H β decay	BE of ^{16,24}O, ^{40,48}Ca
SCGF, Cipollone *et al.*	BE of ^{3}H and ^{4}He, and ^{3}H β decay	BE of ^{13,27}N, ^{14,28}O and ^{15,29}F
AFDMC, Lynn *et al.*	BE of ^{3}H and n-^{4}He P-wave phase shifts	EoS of nucleonic matter
MBPT, Bogner *et al.*, Hebeler *et al.*, Drischler *et al.*, Wienholtz *et al.*, Simonis *et al.*	BE ^{3}H and R_c of ^{4}He	symmetric and asymmetric NM, BE of $^{48-58}$Ca, spectrum of *sd*-shell nuclei with $8 \leq Z, N \leq 20$, BE and R_c of open- and closed-shell nuclei up to $A = 78$
NCCI, Epelbaum *et al.*, Maris *et al.*	BE of ^3H, nd spin-doublet scattering length and the pd differential cross section	the spectrum of light nuclei with $A = 3$–16, elastic nd scattering and in the deuteron breakup reactions, properties of the $A = 3, 4$ nuclei, and for spectra of p-shell nuclei up to $A = 16$, BE and R_c of the oxygen and calcium isotope chains
CC, Carlson *et al.*, Ekström *et al.*, Hagen *et al.*	BE of ^{3}H, ^{3,4}He, ^{14}Li and ^{16,22,24,25}O	R_c and BE of nuclei up to ^{40}Ca, symmetric nuclear matter, neutron skin of ^{48}Ca, structure of ^{78}Ni
NCSM, IM-SRC, IM-NCSM, Hüther *et al.*	BE of ^{3}H and ^{16}O	R_c and BE of ^{4}He, $^{14-26}$O, $^{36-52}$Ca and $^{48-78}$Ni, the spectrum of ^{7}Li, ^{8}Be, ^{9}Be and ^{10}B
CC, Jiang *et al.*	properties of $A \leq 4$	properties of nuclei from $A = 16 - 132$

Beyond exact diagonalization: Euclidean-time projection

For larger many-body systems $\Longleftrightarrow$ Hilbert space grows exponentially.
We need a method that isolates the low-energy states without constructing and diagonalizing the entire many-body matrix.



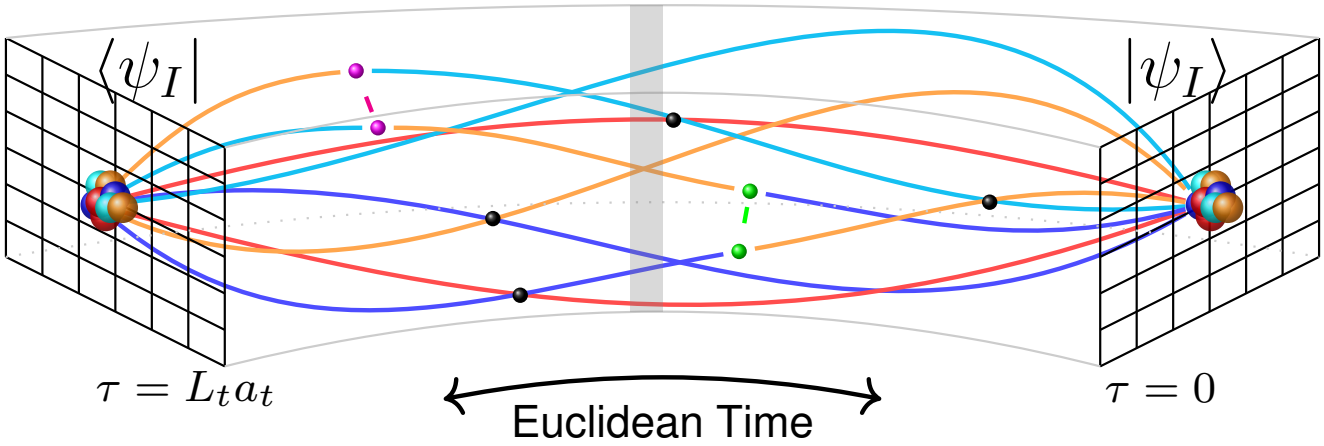
- Define the Euclidean-time evolution operator $M =: e^{-a_t H} :$.
- Construct an initial/final state of nucleons, $|\psi_I\rangle$, as a Slater determinant of free-particle standing waves on the lattice.
- If $H|\Psi_n\rangle = E_n|\Psi_n\rangle \quad \Longrightarrow \quad |\Psi_{\text{trial}}\rangle = \sum_n c_n|\Psi_n\rangle$, and after L_t Euclidean-time steps

$$M^{L_t}|\Psi_{\text{trial}}\rangle = \sum_n c_n e^{-a_t E_n L_t}|\Psi_n\rangle.$$

Since $\cdots > E_2 > E_1 > E_0 \quad \Longrightarrow \quad \lim_{L_t\to\infty} M^{L_t}|\Psi_{\text{trial}}\rangle \propto e^{-a_t E_0 L_t}|\Psi_0\rangle$

Beyond exact diagonalization: Euclidean-time projection

For larger many-body systems $\Longleftrightarrow$ Hilbert space grows exponentially.
We need a method that isolates the low-energy states without constructing and diagonalizing the entire many-body matrix.



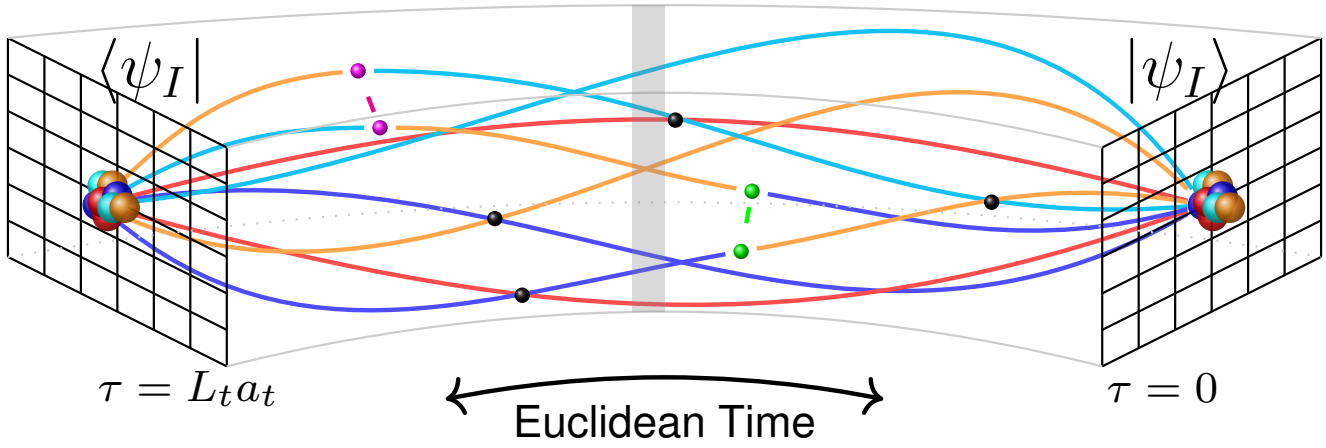
- Define the Euclidean-time evolution operator $M =: e^{-a_t H} :$.
- Construct an initial/final state of nucleons, $|\psi_I\rangle$, as a Slater determinant of free-particle standing waves on the lattice.
- If $H|\Psi_n\rangle = E_n|\Psi_n\rangle \quad \Longrightarrow \quad |\Psi_{\text{trial}}\rangle = \sum_n c_n|\Psi_n\rangle$, and after L_t Euclidean-time steps

$$M^{L_t}|\Psi_{\text{trial}}\rangle = \sum_n c_n e^{-a_t E_n L_t}|\Psi_n\rangle.$$

Since $\cdots > E_2 > E_1 > E_0 \quad \Longrightarrow \quad \lim_{L_t\to\infty} M^{L_t}|\Psi_{\text{trial}}\rangle \propto e^{-a_t E_0 L_t}|\Psi_0\rangle$

Beyond exact diagonalization: Euclidean-time projection

For larger many-body systems $\Longleftrightarrow$ Hilbert space grows exponentially.
We need a method that isolates the low-energy states without constructing and diagonalizing the entire many-body matrix.



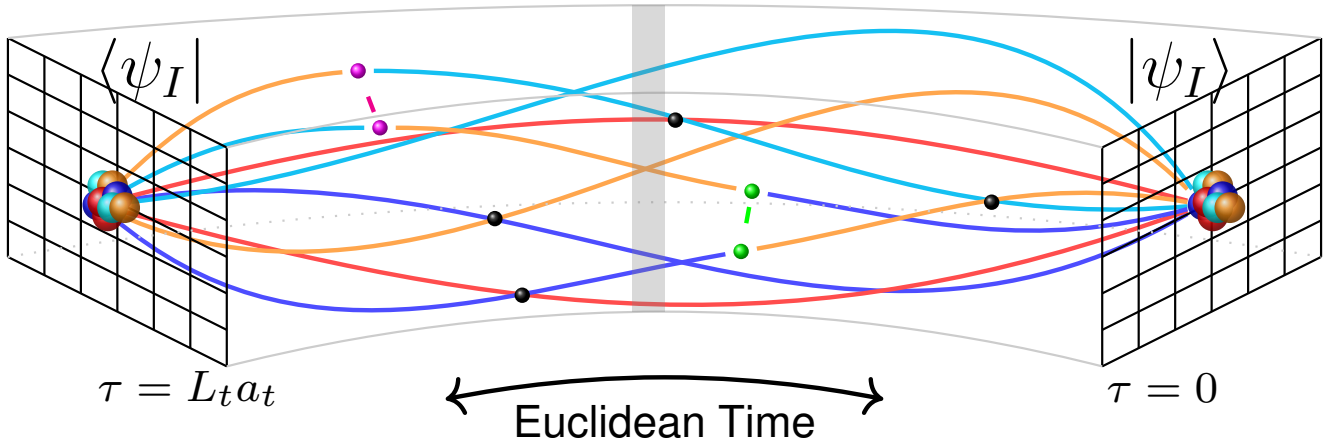
- Define the Euclidean-time evolution operator $M =: e^{-a_t H} :$.
- Construct an initial/final state of nucleons, $|\psi_I\rangle$, as a Slater determinant of free-particle standing waves on the lattice.
- If $H|\Psi_n\rangle = E_n|\Psi_n\rangle \quad \Longrightarrow \quad |\Psi_{\text{trial}}\rangle = \sum_n c_n|\Psi_n\rangle$, and after L_t Euclidean-time steps

$$M^{L_t}|\Psi_{\text{trial}}\rangle = \sum_n c_n e^{-a_t E_n L_t}|\Psi_n\rangle.$$

Since $\cdots > E_2 > E_1 > E_0 \quad \Longrightarrow \quad \lim_{L_t\to\infty} M^{L_t}|\Psi_{\text{trial}}\rangle \propto e^{-a_t E_0 L_t}|\Psi_0\rangle$

Beyond exact diagonalization: Euclidean-time projection

For larger many-body systems $\Longleftrightarrow$ Hilbert space grows exponentially.
We need a method that isolates the low-energy states without constructing and diagonalizing the entire many-body matrix.



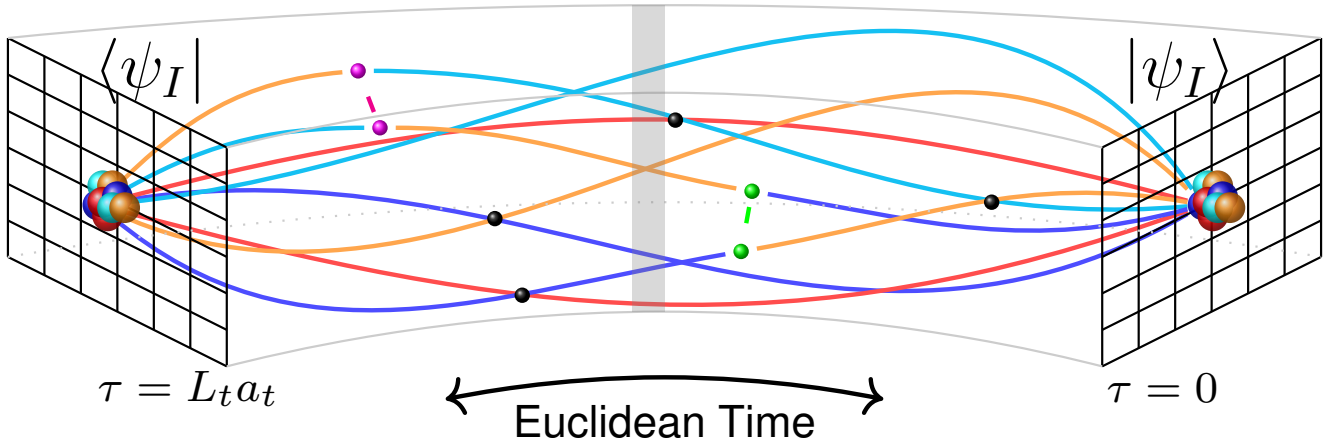
- Define the Euclidean-time evolution operator $M =: e^{-a_t H} :$.
- Construct an initial/final state of nucleons, $|\psi_I\rangle$, as a Slater determinant of free-particle standing waves on the lattice.
- If $H|\Psi_n\rangle = E_n|\Psi_n\rangle \quad \Longrightarrow \quad |\Psi_{\text{trial}}\rangle = \sum_n c_n|\Psi_n\rangle$, and after L_t Euclidean-time steps

$$M^{L_t}|\Psi_{\text{trial}}\rangle = \sum_n c_n e^{-a_t E_n L_t}|\Psi_n\rangle.$$

Since $\cdots > E_2 > E_1 > E_0 \quad \Longrightarrow \quad \lim_{L_t\to\infty} M^{L_t}|\Psi_{\text{trial}}\rangle \propto e^{-a_t E_0 L_t}|\Psi_0\rangle$

Beyond exact diagonalization: Euclidean-time projection

For larger many-body systems $\Longleftrightarrow$ Hilbert space grows exponentially.
We need a method that isolates the low-energy states without constructing and diagonalizing the entire many-body matrix.



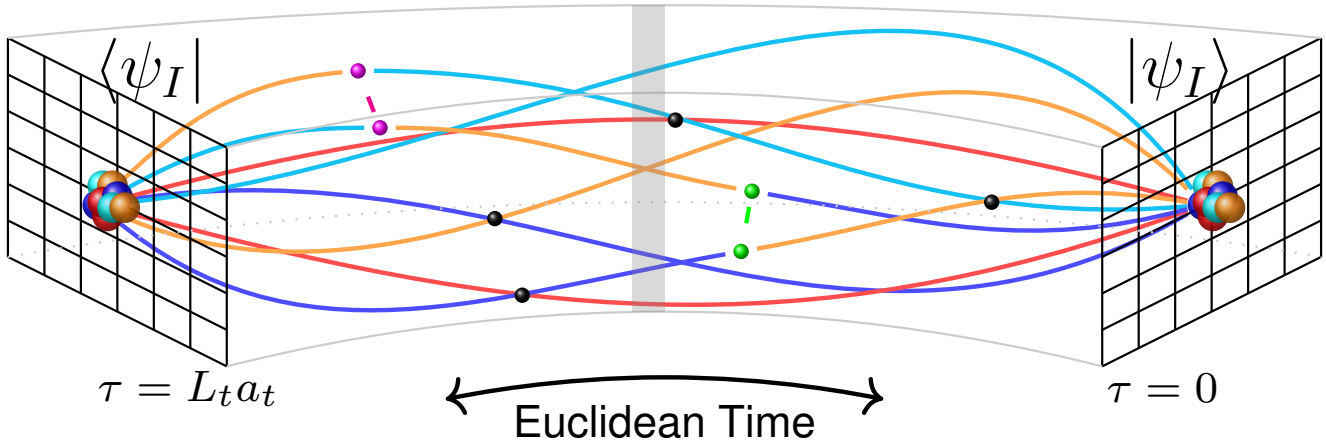
- Define the Euclidean-time evolution operator $M =: e^{-a_t H} :$.
- Construct an initial/final state of nucleons, $|\psi_I\rangle$, as a Slater determinant of free-particle standing waves on the lattice.
- If $H|\Psi_n\rangle = E_n|\Psi_n\rangle \quad \Longrightarrow \quad |\Psi_{\text{trial}}\rangle = \sum_n c_n|\Psi_n\rangle$, and after L_t Euclidean-time steps

$$\boxed{M^{L_t}|\Psi_{\text{trial}}\rangle = \sum_n c_n e^{-a_t E_n L_t}|\Psi_n\rangle.}$$

Since $\cdots > E_2 > E_1 > E_0 \quad \Longrightarrow \quad \lim_{L_t\to\infty} M^{L_t}|\Psi_{\text{trial}}\rangle \propto e^{-a_t E_0 L_t}|\Psi_0\rangle$

Beyond exact diagonalization: Euclidean-time projection

For larger many-body systems $\Longleftrightarrow$ Hilbert space grows exponentially.
We need a method that isolates the low-energy states without constructing and diagonalizing the entire many-body matrix.



- Define the Euclidean-time evolution operator $M =: e^{-a_t H} :$.
- Construct an initial/final state of nucleons, $|\psi_I\rangle$, as a Slater determinant of free-particle standing waves on the lattice.
- If $H|\Psi_n\rangle = E_n|\Psi_n\rangle \quad \Longrightarrow \quad |\Psi_{\text{trial}}\rangle = \sum_n c_n|\Psi_n\rangle$, and after L_t Euclidean-time steps

$$\boxed{M^{L_t}|\Psi_{\text{trial}}\rangle = \sum_n c_n e^{-a_t E_n L_t}|\Psi_n\rangle.}$$

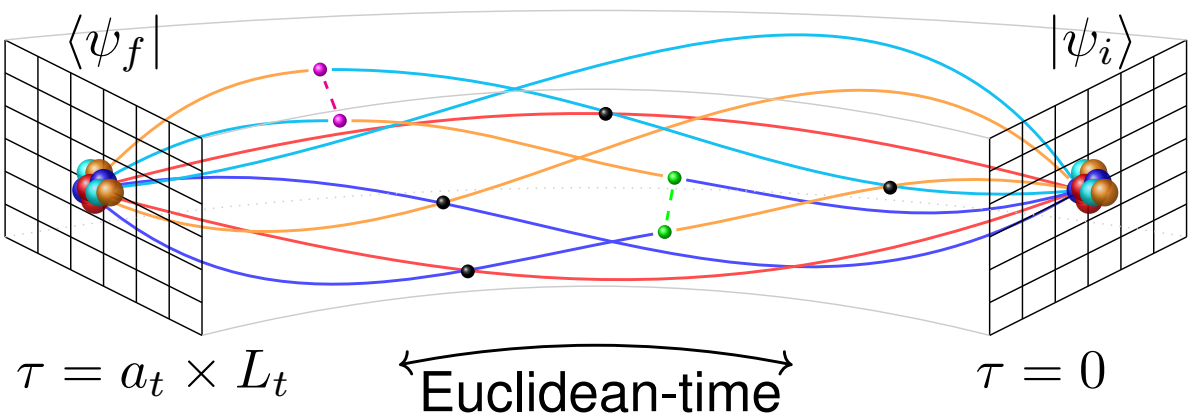
Since $\cdots > E_2 > E_1 > E_0 \quad \Longrightarrow \quad \lim_{L_t\to\infty} M^{L_t}|\Psi_{\text{trial}}\rangle \propto e^{-a_t E_0 L_t}|\Psi_0\rangle$

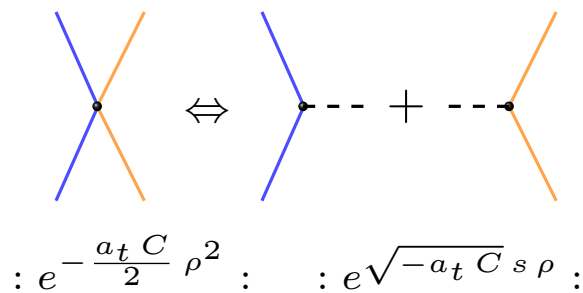
Auxiliary field Monte Carlo

Use a Gaussian integral identity

$$\exp\left[-\frac{C}{2}\,\rho^2\right] = \sqrt{\frac{1}{2\pi}}\int ds\, \exp\left[-\frac{s^2}{2} + \sqrt{-C}\, s\, \rho\right]$$

s is an auxiliary field coupled to the particle density. Each nucleon evolves as if a single particle in a fluctuating background of pion fields and auxiliary fields.





Lattice Monte Carlo calculations: Euclidean time projection

- Start from an initial state $|\psi_I\rangle$ with the desired quantum numbers.
- Project with the reference/sign-friendly Hamiltonian $H_S \Longleftrightarrow$ a product of a string of transfer matrix $M_S =: \exp(-a_t H_S) :$,

$$|\psi_S^{(0)}\rangle = \lim_{L_t \to \infty} M_S^{L_t/2} |\psi_I\rangle, \qquad \tau = L_t a_t.$$

- Define the projected amplitudes

$$\mathcal{M}(\mathcal{O}) = \langle \psi_I | M_S^{L_t/2} \, \mathcal{O} \, M_S^{L_t/2} | \psi_I \rangle.$$

- The ground state energy of non-perturbative Hamiltonian

$$E_S^{(0)} = \frac{\mathcal{M}(H_S)}{\mathcal{M}(1)}.$$

- First-order perturbative higher order correction

$$V_C = H_\chi - H_S, \qquad \delta E_1 = \frac{\mathcal{M}(V_C)}{\mathcal{M}(1)}, \qquad E_1 = E_S^{(0)} + \delta E_1.$$

Lattice Monte Carlo calculations: Euclidean time projection

- Start from an initial state $|\psi_I\rangle$ with the desired quantum numbers.
- Project with the reference/sign-friendly Hamiltonian $H_S \Longleftrightarrow$ a product of a string of transfer matrix $M_S =: \exp(-a_t H_S) :$,

$$|\psi_S^{(0)}\rangle = \lim_{L_t \to \infty} M_S^{L_t/2} |\psi_I\rangle, \qquad \tau = L_t a_t.$$

- Define the projected amplitudes

$$\mathcal{M}(\mathcal{O}) = \langle \psi_I | M_S^{L_t/2} \, \mathcal{O} \, M_S^{L_t/2} | \psi_I \rangle.$$

- The ground state energy of non-perturbative Hamiltonian

$$E_S^{(0)} = \frac{\mathcal{M}(H_S)}{\mathcal{M}(1)}.$$

- First-order perturbative higher order correction

$$V_C = H_\chi - H_S, \qquad \delta E_1 = \frac{\mathcal{M}(V_C)}{\mathcal{M}(1)}, \qquad E_1 = E_S^{(0)} + \delta E_1.$$

Lattice Monte Carlo calculations: Euclidean time projection

- Start from an initial state $|\psi_I\rangle$ with the desired quantum numbers.
- Project with the reference/sign-friendly Hamiltonian $H_S \Longleftrightarrow$ a product of a string of transfer matrix $M_S =: \exp(-a_t H_S) :$,

$$|\psi_S^{(0)}\rangle = \lim_{L_t \to \infty} M_S^{L_t/2} |\psi_I\rangle, \qquad \tau = L_t a_t.$$

- Define the projected amplitudes

$$\mathcal{M}(\mathcal{O}) = \langle \psi_I | M_S^{L_t/2} \, \mathcal{O} \, M_S^{L_t/2} | \psi_I \rangle.$$

- The ground state energy of non-perturbative Hamiltonian

$$E_S^{(0)} = \frac{\mathcal{M}(H_S)}{\mathcal{M}(1)}.$$

- First-order perturbative higher order correction

$$V_C = H_\chi - H_S, \qquad \delta E_1 = \frac{\mathcal{M}(V_C)}{\mathcal{M}(1)}, \qquad E_1 = E_S^{(0)} + \delta E_1.$$

Lattice Monte Carlo calculations: Euclidean time projection

- Start from an initial state $|\psi_I\rangle$ with the desired quantum numbers.
- Project with the reference/sign-friendly Hamiltonian $H_S \Longleftrightarrow$ a product of a string of transfer matrix $M_S =: \exp(-a_t H_S) :$,

$$|\psi_S^{(0)}\rangle = \lim_{L_t \to \infty} M_S^{L_t/2} |\psi_I\rangle, \qquad \tau = L_t a_t.$$

- Define the projected amplitudes

$$\mathcal{M}(\mathcal{O}) = \langle \psi_I | M_S^{L_t/2} \, \mathcal{O} \, M_S^{L_t/2} | \psi_I \rangle.$$

- The ground state energy of non-perturbative Hamiltonian

$$E_S^{(0)} = \frac{\mathcal{M}(H_S)}{\mathcal{M}(1)}.$$

- First-order perturbative higher order correction

$$V_C = H_\chi - H_S, \qquad \delta E_1 = \frac{\mathcal{M}(V_C)}{\mathcal{M}(1)}, \qquad E_1 = E_S^{(0)} + \delta E_1.$$

Lattice Monte Carlo calculations: Euclidean time projection

- Start from an initial state $|\psi_I\rangle$ with the desired quantum numbers.
- Project with the reference/sign-friendly Hamiltonian $H_S \Longleftrightarrow$ a product of a string of transfer matrix $M_S =: \exp(-a_t H_S) :$,

$$|\psi_S^{(0)}\rangle = \lim_{L_t \to \infty} M_S^{L_t/2} |\psi_I\rangle, \qquad \tau = L_t a_t.$$

- Define the projected amplitudes

$$\mathcal{M}(\mathcal{O}) = \langle \psi_I | M_S^{L_t/2} \, \mathcal{O} \, M_S^{L_t/2} | \psi_I \rangle.$$

- The ground state energy of non-perturbative Hamiltonian

$$E_S^{(0)} = \frac{\mathcal{M}(H_S)}{\mathcal{M}(1)}.$$

- First-order perturbative higher order correction

$$V_C = H_\chi - H_S, \qquad \delta E_1 = \frac{\mathcal{M}(V_C)}{\mathcal{M}(1)}, \qquad E_1 = E_S^{(0)} + \delta E_1.$$

Euclidean-time projection: Perturbative quantum MC (ptQMC)

- Estimate the wave function using projection MC via transfer matrices $M_S =: \exp(-a_t H_S) :$ and $M_\chi =: \exp(-a_t H_\chi) :$

$$|\psi\rangle = \lim_{L_t\to\infty} M_S^{L_t/2}|\psi_I\rangle = |\psi_S^{(0)}\rangle + |\delta\psi_1\rangle + \mathcal{O}(V_C^2),$$

$$|\delta\psi_1\rangle = \lim_{L_t\to\infty} \sum_{k=1}^{L_t/2} M_S^{L_t/2-k}\,(M_\chi - M_S)\,M_S^{k-1}|\psi_I\rangle.$$

$|\delta\psi_1\rangle$ is the first-order response of the projected state.

- Second-order perturbative higher order correction

$$\delta E_2 = \frac{\mathrm{Re}\Big[\langle\psi_S^{(0)}|(H_\chi - H_S)|\delta\psi_1\rangle - \delta E_1\,\langle\psi_S^{(0)}|\delta\psi_1\rangle\Big]}{\langle\psi_S^{(0)}|\psi_S^{(0)}\rangle},$$

$$E_2 = E_S^{(0)} + \delta E_1 + \delta E_2.$$

No explicit sum over excited states is required.

Lu, Li, SE, Ma, Lee, Meißner, PRL 128, 242501 (2022).

Euclidean-time projection: Perturbative quantum MC (ptQMC)

- Estimate the wave function using projection MC via transfer matrices $M_S =: \exp(-a_t H_S)$: and $M_\chi =: \exp(-a_t H_\chi)$:

$$|\psi\rangle = \lim_{L_t\to\infty} M_S^{L_t/2}|\psi_I\rangle = |\psi_S^{(0)}\rangle + |\delta\psi_1\rangle + \mathcal{O}(V_C^2),$$

$$|\delta\psi_1\rangle = \lim_{L_t\to\infty} \sum_{k=1}^{L_t/2} M_S^{L_t/2-k}\,(M_\chi - M_S)\,M_S^{k-1}|\psi_I\rangle.$$

$|\delta\psi_1\rangle$ is the first-order response of the projected state.

- Second-order perturbative higher order correction

$$\delta E_2 = \frac{\mathrm{Re}\Big[\langle\psi_S^{(0)}|(H_\chi - H_S)|\delta\psi_1\rangle - \delta E_1\,\langle\psi_S^{(0)}|\delta\psi_1\rangle\Big]}{\langle\psi_S^{(0)}|\psi_S^{(0)}\rangle},$$

$$E_2 = E_S^{(0)} + \delta E_1 + \delta E_2.$$

No explicit sum over excited states is required.

Lu, Li, SE, Ma, Lee, Meißner, PRL 128, 242501 (2022).

Euclidean-time projection: Perturbative quantum MC (ptQMC)

- Estimate the wave function using projection MC via transfer matrices $M_S =: \exp(-a_t H_S)$: and $M_\chi =: \exp(-a_t H_\chi)$:

$$|\psi\rangle = \lim_{L_t\to\infty} M_S^{L_t/2}|\psi_I\rangle = |\psi_S^{(0)}\rangle + |\delta\psi_1\rangle + \mathcal{O}(V_C^2),$$

$$|\delta\psi_1\rangle = \lim_{L_t\to\infty} \sum_{k=1}^{L_t/2} M_S^{L_t/2-k}\,(M_\chi - M_S)\,M_S^{k-1}|\psi_I\rangle.$$

$|\delta\psi_1\rangle$ is the first-order response of the projected state.

- Second-order perturbative higher order correction

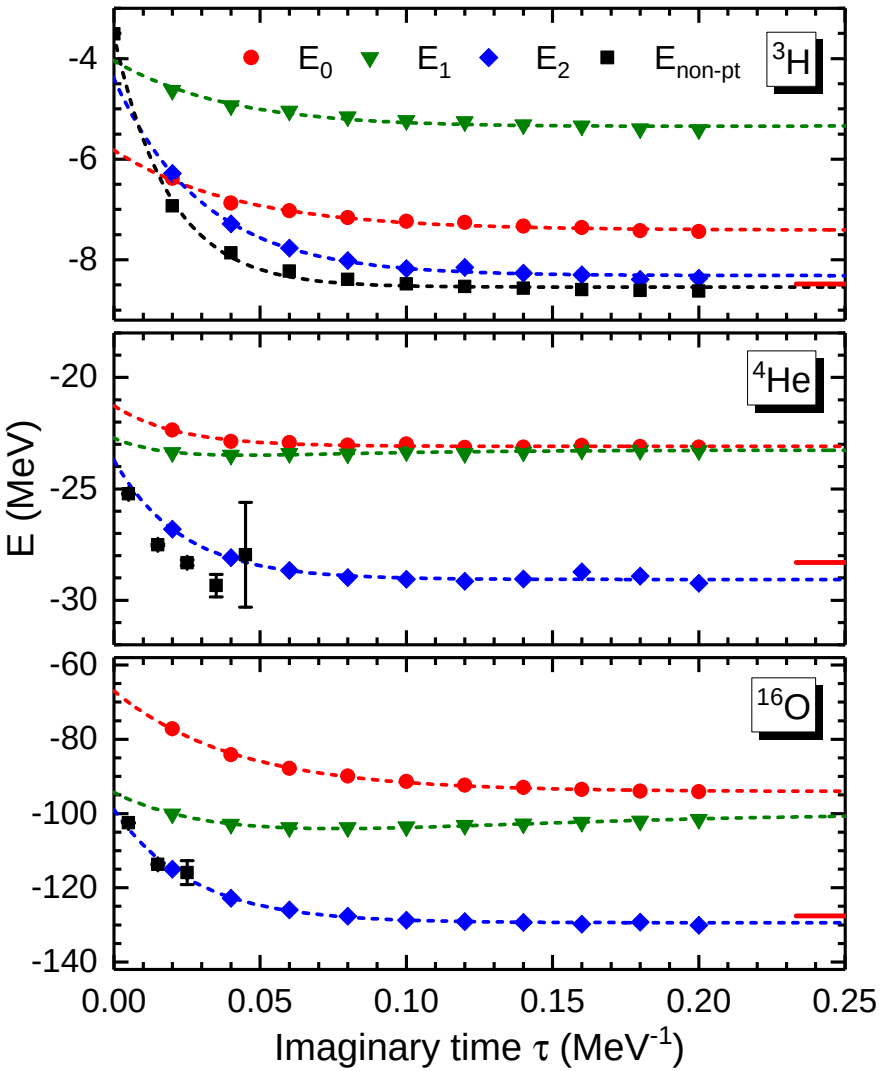
$$\delta E_2 = \frac{\mathrm{Re}\Big[\langle\psi_S^{(0)}|(H_\chi - H_S)|\delta\psi_1\rangle - \delta E_1\,\langle\psi_S^{(0)}|\delta\psi_1\rangle\Big]}{\langle\psi_S^{(0)}|\psi_S^{(0)}\rangle},$$

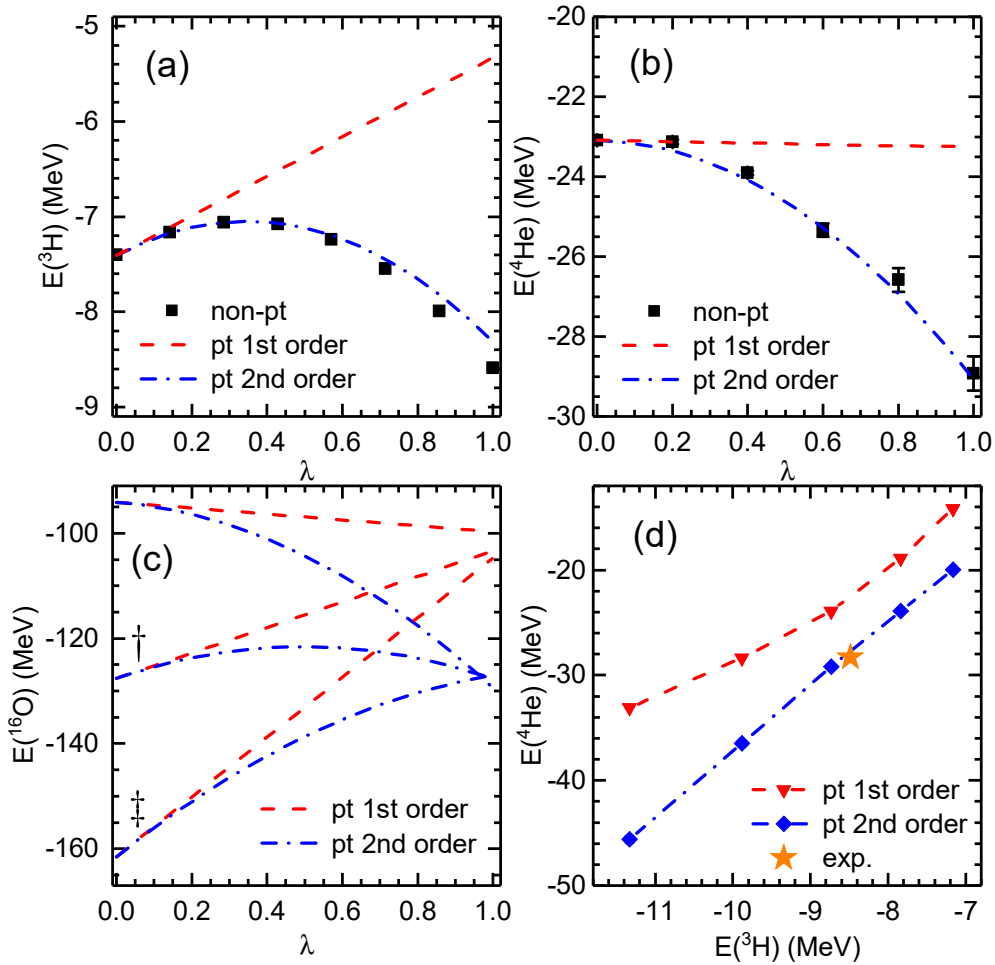
$$E_2 = E_S^{(0)} + \delta E_1 + \delta E_2.$$

No explicit sum over excited states is required.

Lu, Li, SE, Ma, Lee, Meißner, PRL 128, 242501 (2022).

Perturbative quantum MC (ptQMC)





$$H = H_S + \lambda\,(H_\chi - H_S)$$

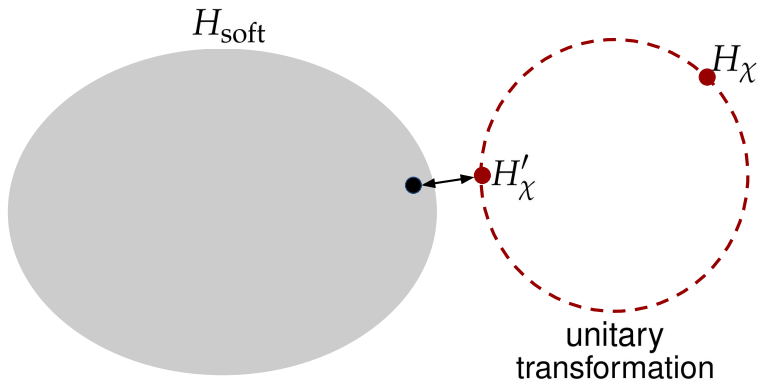
Lu, Li, SE, Ma, Lee, Meißner, PRL 128, 242501 (2022).

Wavefunction Matching

- H_χ : –severe sign oscillation, –derived from the underlying theory.
- $H_{\rm soft}$: –tolerable sign oscillation, –many-body observables with a fair agreement.

Can unitary transformation create a new chiral Hamiltonian which is (first order) perturbation theory friendly?

$$H'_\chi = U^\dagger H_\chi U$$



- Let $|\psi^0_\chi\rangle$ be the normalized lowest eigenstate of H_χ.
- Let $|\psi^0_{\rm soft}\rangle$ be the normalized lowest eigenstate of $H_{\rm soft}$.

$$U_{R',R} = \theta(r-R)\,\delta_{R',R} + \theta(R'-r)\,\theta(R-r)\;|\psi^\perp_\chi\rangle\,\langle\psi^\perp_{\rm soft}|$$

A perturbative-friendly Hamiltonian H'_χ via wavefunction matching $\rightarrow$

$$H'_\chi = H_{\rm soft} + \boxed{(H'_\chi - H_{\rm soft})}$$

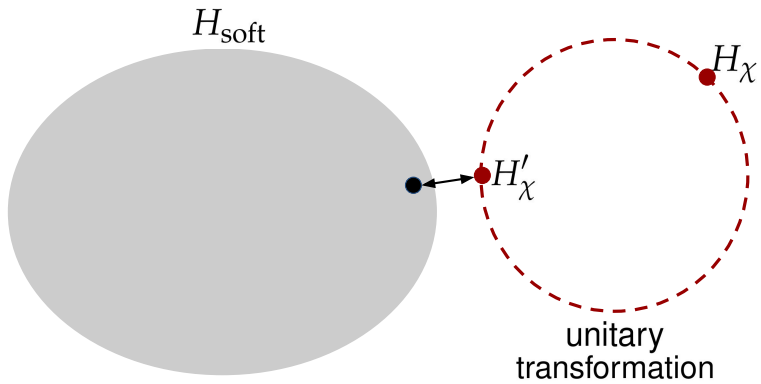
SE et al. *Nature* 630, 8015, 59-63 (2024)

Wavefunction Matching

- H_χ : –severe sign oscillation, –derived from the underlying theory.
- $H_{\rm soft}$: –tolerable sign oscillation, –many-body observables with a fair agreement.

Can unitary transformation create a new chiral Hamiltonian which is (first order) perturbation theory friendly?

$$H'_\chi = U^\dagger H_\chi U$$



- Let $|\psi^0_\chi\rangle$ be the normalized lowest eigenstate of H_χ.
- Let $|\psi^0_{\rm soft}\rangle$ be the normalized lowest eigenstate of $H_{\rm soft}$.

$$U_{R',R} = \theta(r-R)\,\delta_{R',R} + \theta(R'-r)\,\theta(R-r)\;|\psi^\perp_\chi\rangle\,\langle\psi^\perp_{\rm soft}|$$

A perturbative-friendly Hamiltonian H'_χ via wavefunction matching $\rightarrow$

$$H'_\chi = H_{\rm soft} + \boxed{(H'_\chi - H_{\rm soft})}$$

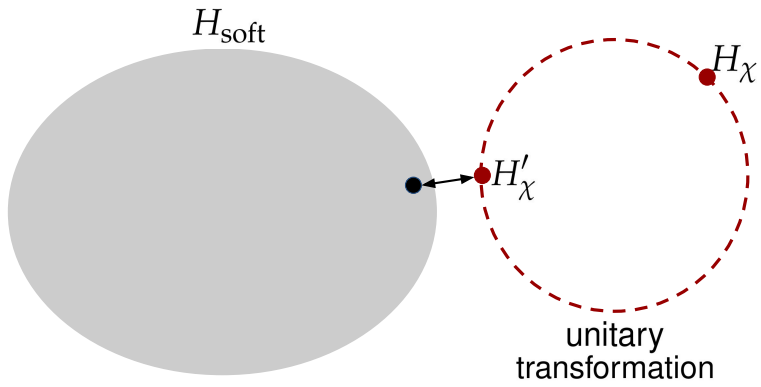
SE et al. *Nature* 630, 8015, 59-63 (2024)

Wavefunction Matching

- H_χ : –severe sign oscillation, –derived from the underlying theory.
- $H_{\rm soft}$: –tolerable sign oscillation, –many-body observables with a fair agreement.

Can unitary transformation create a new chiral Hamiltonian which is (first order) perturbation theory friendly?

$$H'_\chi = U^\dagger\, H_\chi\, U$$



- Let $|\psi^0_\chi\rangle$ be the normalized lowest eigenstate of H_χ.
- Let $|\psi^0_{\rm soft}\rangle$ be the normalized lowest eigenstate of $H_{\rm soft}$.

$$U_{R',R} = \theta(r-R)\,\delta_{R',R} + \theta(R'-r)\,\theta(R-r)\;|\psi^\perp_\chi\rangle\,\langle\psi^\perp_{\rm soft}|$$

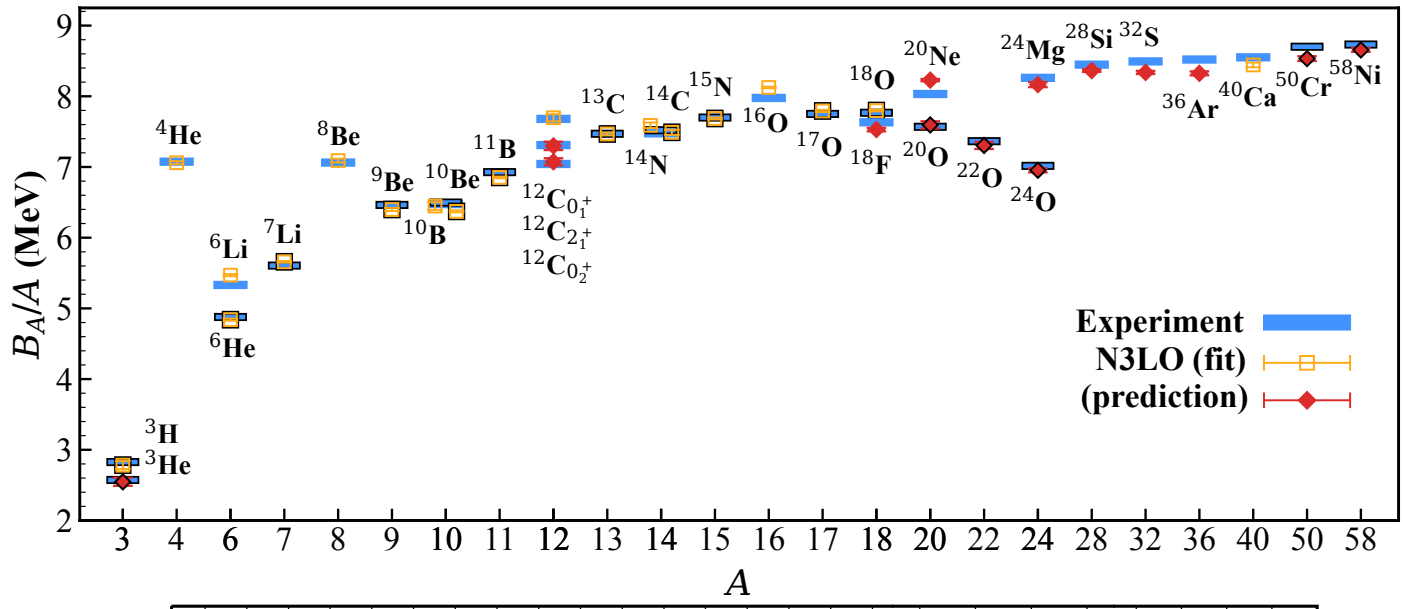
A perturbative-friendly Hamiltonian H'_χ via wavefunction matching $\rightarrow$

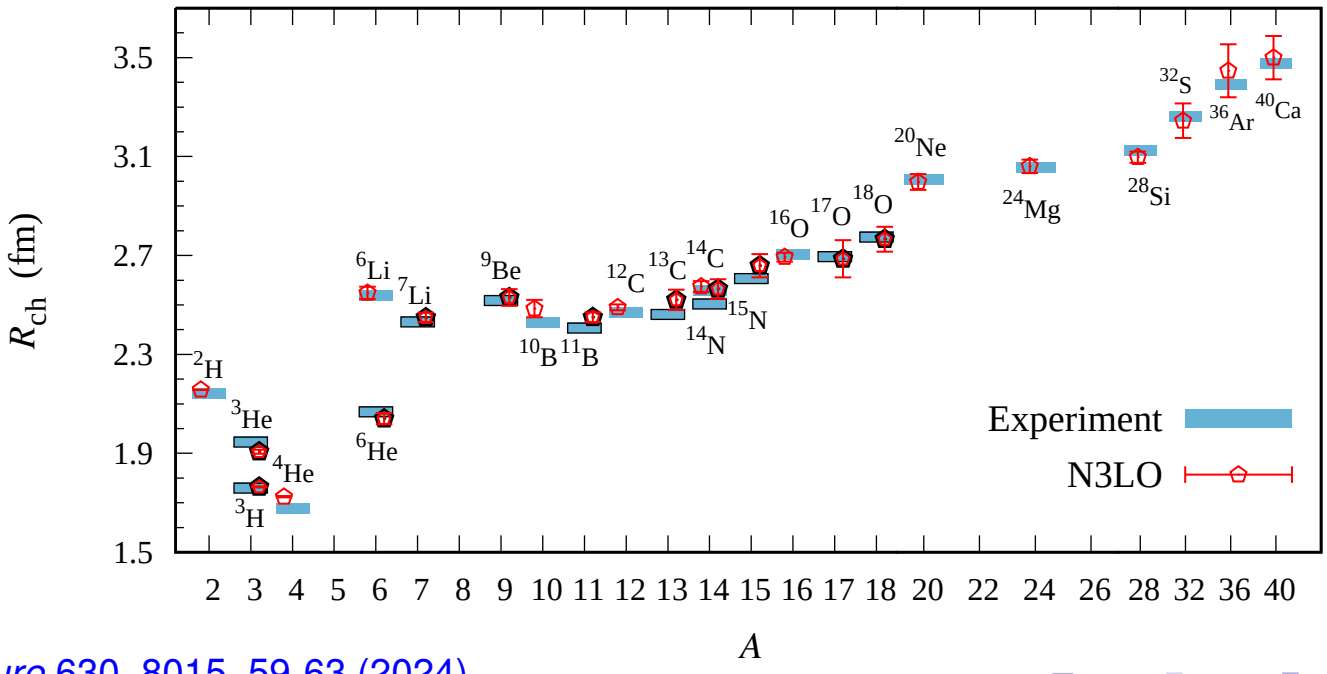
$$H'_\chi = H_{\rm soft} + \boxed{(H'_\chi - H_{\rm soft})}$$

SE et al. *Nature* 630, 8015, 59-63 (2024)

Ab initio nuclear theory: recent progress in NLEFT

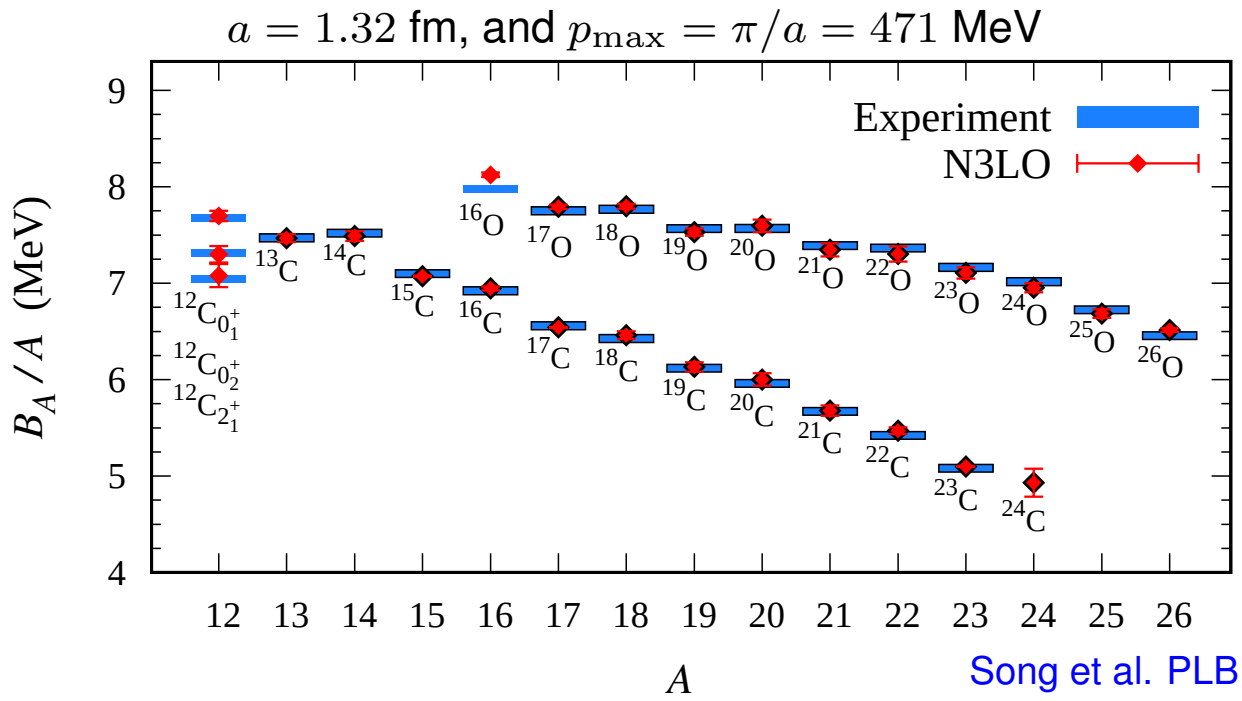
$a = 1.32$ fm and $p_{\max} = \pi/a = 471$ MeV



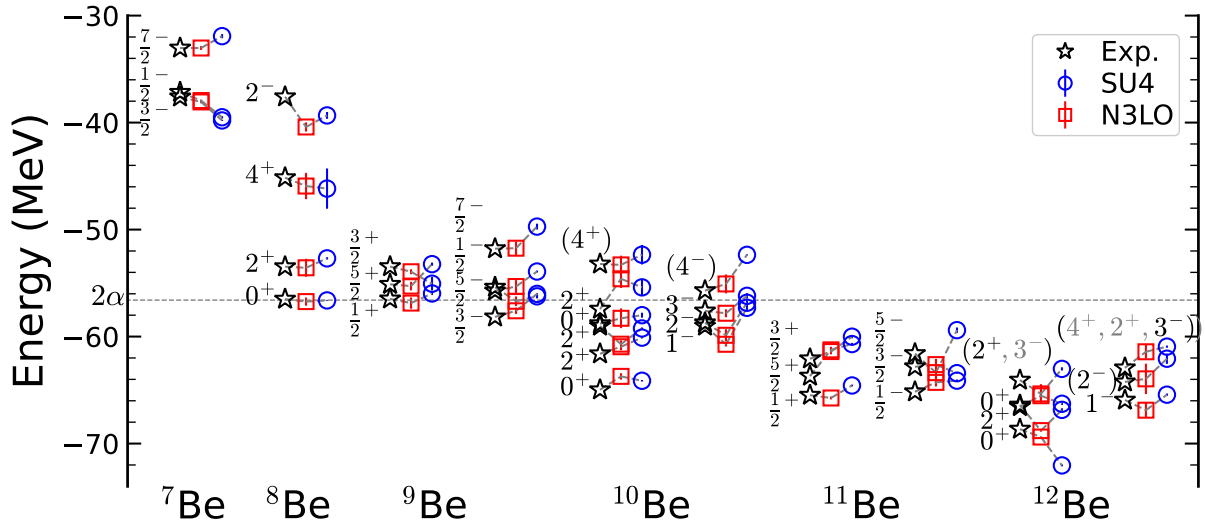


SE et al. *Nature* 630, 8015, 59-63 (2024)

Ab initio nuclear theory: recent progress in NLEFT



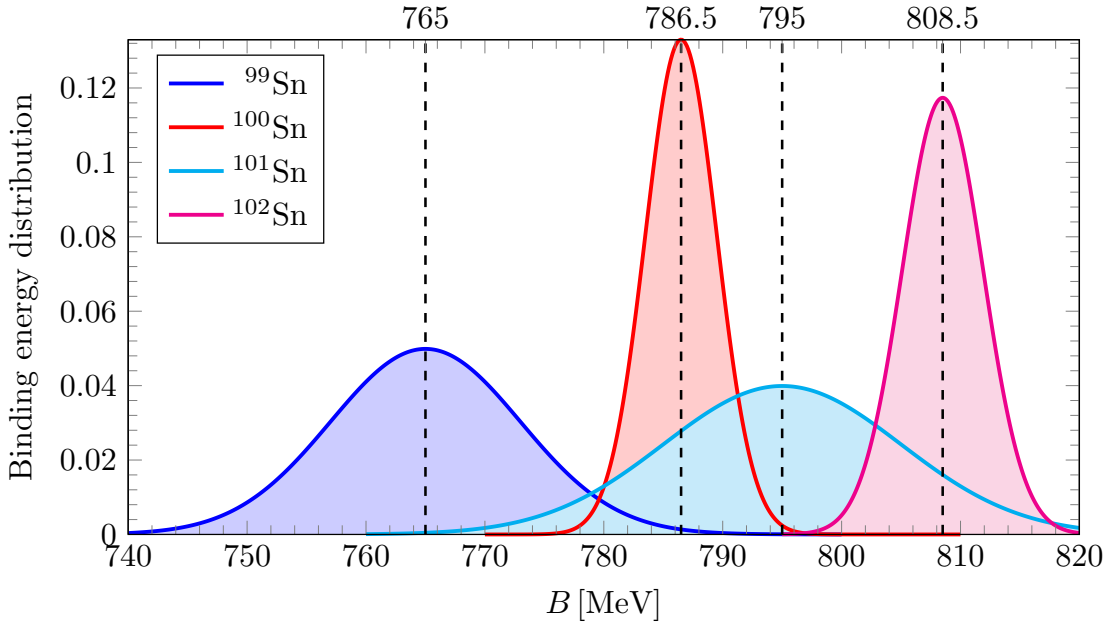
Song et al. PLB 872 (2026) 140086



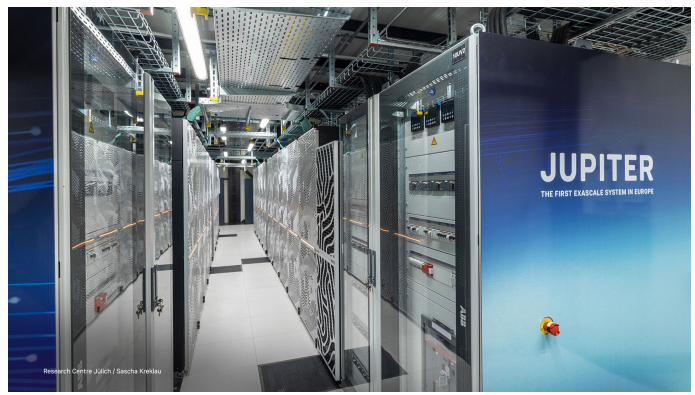
Shen, SE, Lee, Meißner, Ren PRL 134 (2025) 16, 162503

Ab initio nuclear theory: recent progress in NLEFT

$a = 1.32$ fm, and $p_{\max} = \pi/a = 471$ MeV



Isotopes	N^{3}LO	N^{3}LO*	Exp.
$102 - 101$	13.5 ± 10.6	14.1 ± 10.6	12.7 ± 0.3
$102 - 100^\star$	22.5 ± 4.6	22.9 ± 4.6	23.9 ± 0.3
$102 - 99$	43.5 ± 8.7	44.1 ± 8.7	41.2 ± 0.6
$101 - 100$	8.5 ± 10.4	8.9 ± 10.4	11.2 ± 0.4
$101 - 99^\star$	30.0 ± 12.8	30.1 ± 12.8	28.5 ± 0.7
$100 - 99$	21.5 ± 8.6	21.2 ± 8.6	17.3 ± 0.7

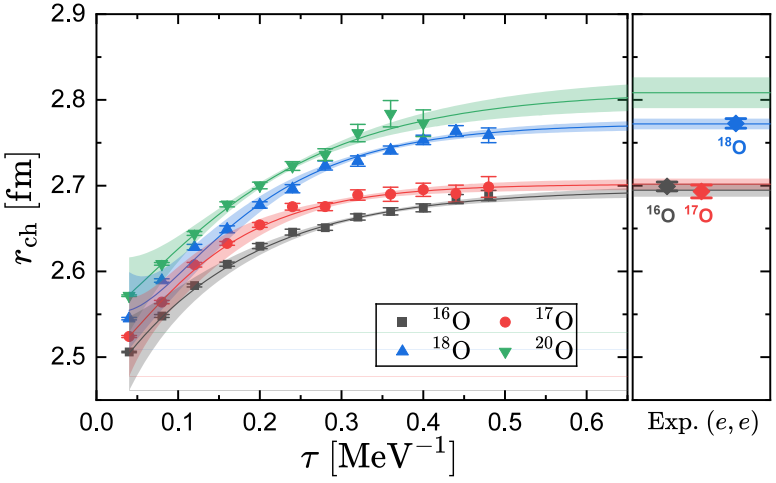


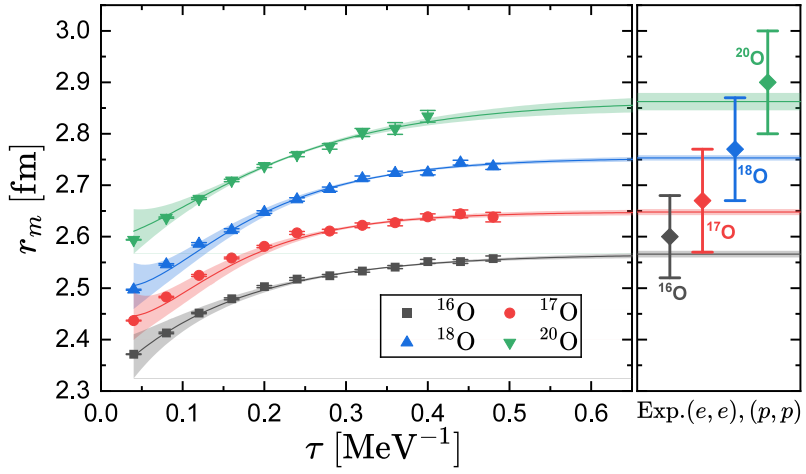
Large-scale GPU programming for Exascale supercomputer.

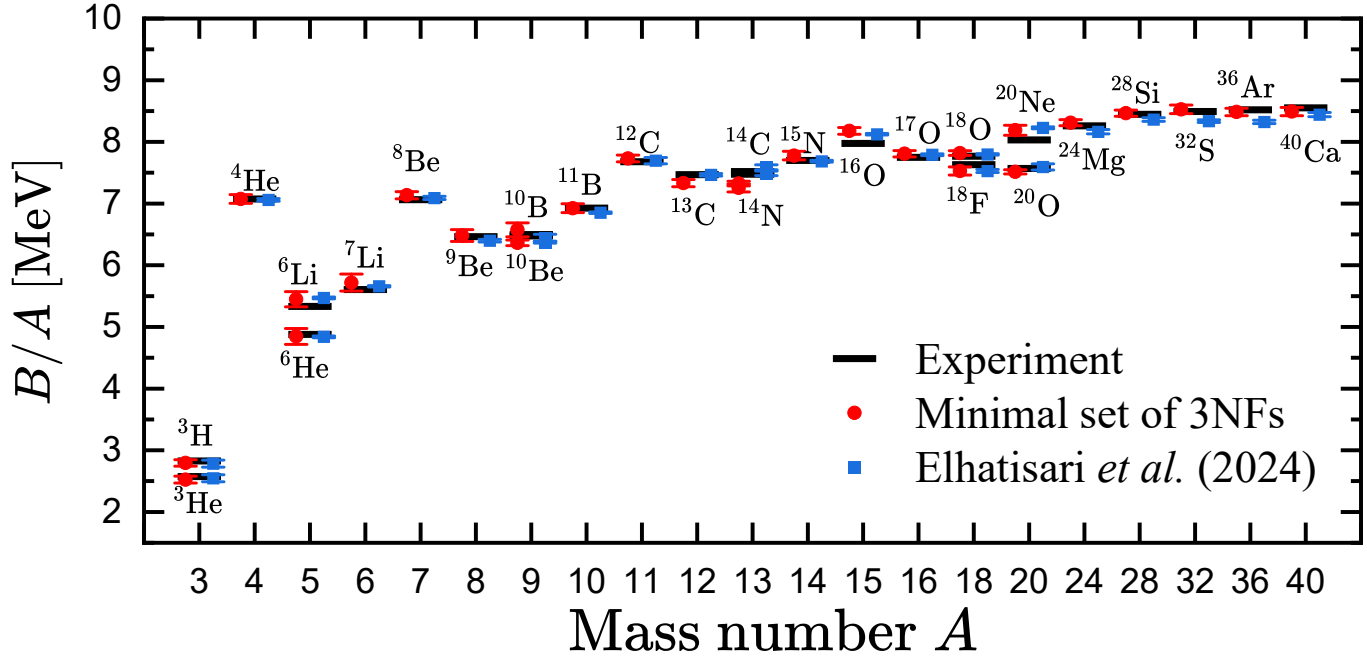
Hildenbrand, SE, Meißner, Meyer, Ren, Herten, Bode PRL 136 (2026) 6, 062501

Ab initio nuclear theory: recent progress in NLEFT

$a = 1.32$ fm, and $p_{\max} = \pi/a = 471$ MeV







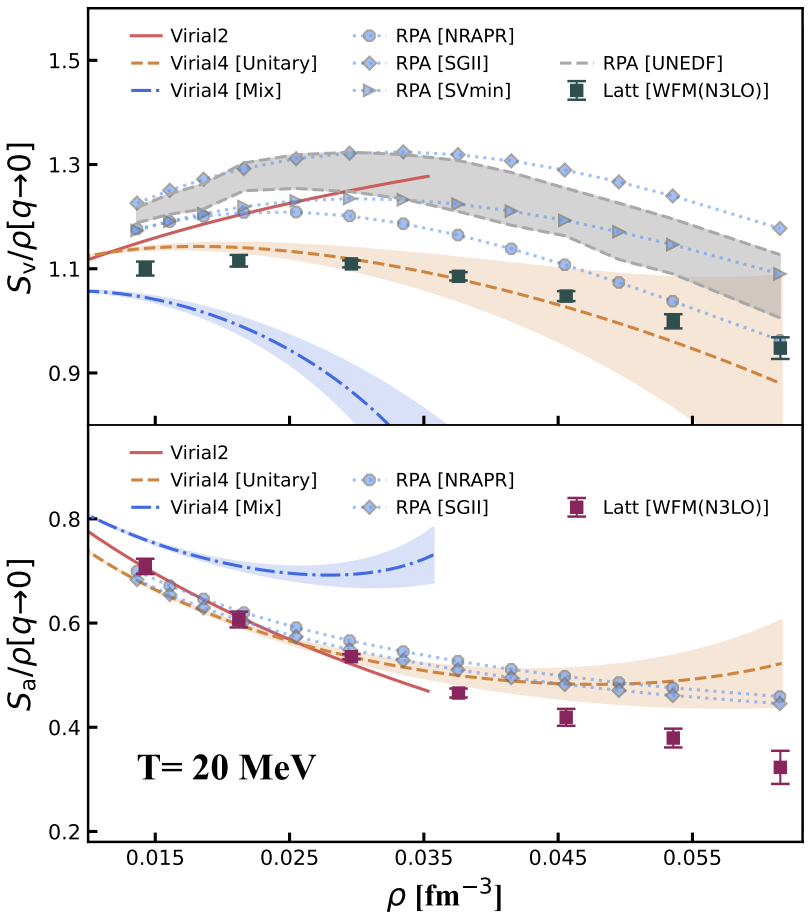
Ren, SE, Meißner PRL 135 (2025) 15, 152502

Ab initio nuclear theory: recent results at N3LO

Structure Factors for Hot Neutron Matter:

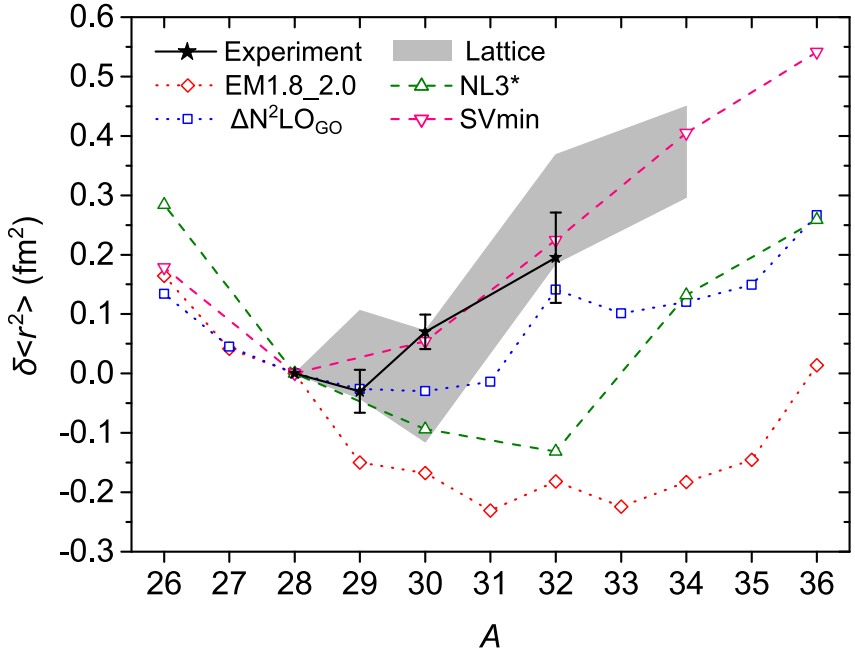
$$S_{\rm v}(\vec{q}) = \frac{1}{L^3}\sum_{\vec{n}\vec{n}'} {\rm e}^{-i\vec{q}\cdot\vec{n}}\left[\langle\hat{\rho}(\vec{n}+\vec{n}')\hat{\rho}(\vec{n}')\rangle - (\rho^0)^2\right],$$

$$S_{\rm a}(\vec{q}) = \frac{1}{L^3}\sum_{\vec{n}\vec{n}'} {\rm e}^{-i\vec{q}\cdot\vec{n}}\left[\langle\hat{\rho}_z(\vec{n}+\vec{n}')\hat{\rho}_z(\vec{n}')\rangle - (\rho_z^0)^2\right],$$



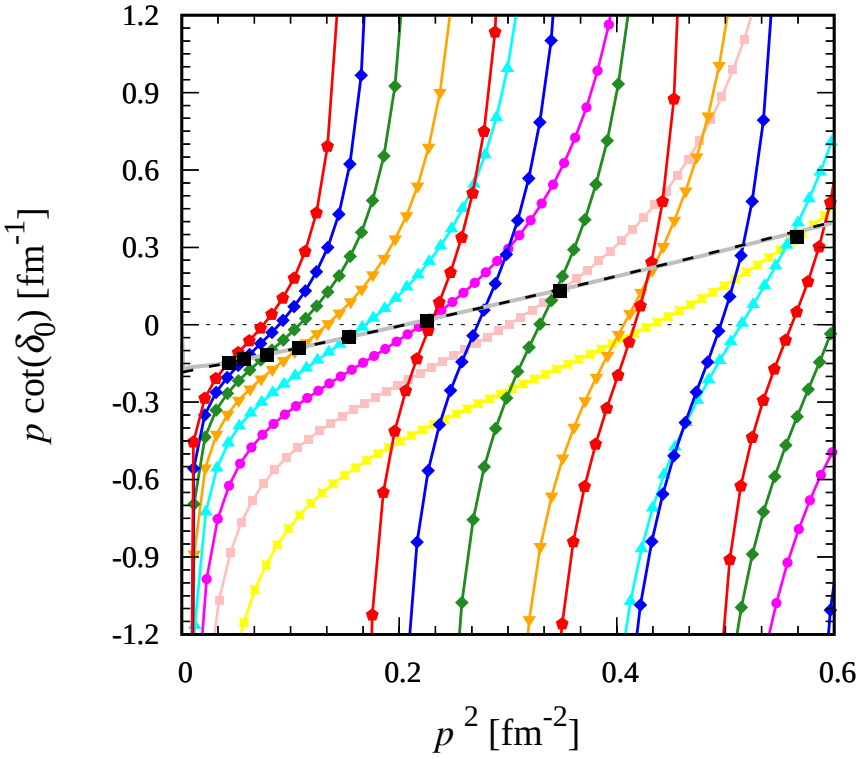
Ma et al., PRL 132 (2024) 23, 232502

Nuclear charge radii of silicon isotopes:



Koenig et al., PRL 132 (2024) 16, 162502

Scattering on the lattice



$$p\cot\delta_0(p) = \frac{1}{\pi L}\left[\sum_{\vec{n}}^{\Lambda}\frac{\theta\left(\Lambda^2-\vec{n}^2\right)}{\vec{n}^2-(Lp/2\pi)^2} - 4\pi\,\Lambda\right]$$

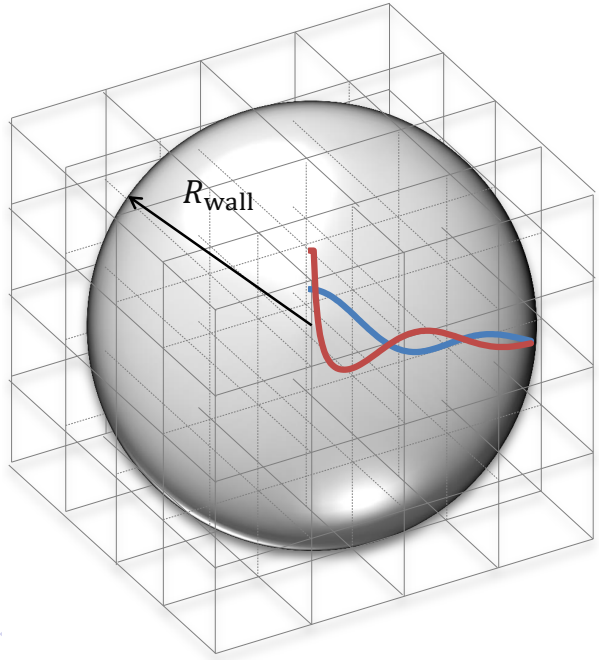
Lüscher's finite volume method:

Lüscher, Comm. Math. Phys. 105 (1986) 153; NPB 354 (1991) 531

Spherical wall method:

$$R_\ell^{(p)}(r) = N_\ell(p)\times\begin{cases}\cot\delta_\ell(p)\,j_\ell(p\,r) - n_\ell(p\,r)\\ \cot\delta_\ell(p)\,F_\ell(p\,r) + G_\ell(p\,r)\end{cases}$$

Nucl. Phys. A 424, 47-59 (1984), Eur. Phys. J. A 34, 185-196 (2007).



Two ways to extract scattering phase shifts on the lattice

Lüscher's method

Keep the **periodic cubic box** and calculate its discrete energy spectrum,

$$E_n(L_{\rm box}).$$

The periodic-box geometry is encoded in

$$\boxed{p\cot\delta_0(p) = \frac{1}{\pi L_{\rm box}} S(\eta), \qquad \eta = \left(\frac{pL_{\rm box}}{2\pi}\right)^2}$$

Therefore,

$$\boxed{E_n(L_{\rm box}) \longrightarrow p_n \longrightarrow \delta_0(p_n).}$$

The scattering information is extracted from **the energy spectrum**.

Spherical-wall method

Replace the periodic boundary condition on the relative motion by a **spherical wall**,

$$R_\ell(R_W) = 0, \qquad R_W > R_{\rm int}.$$

$$R_\ell(r) \simeq A h_\ell^{(-)}(pr) - B h_\ell^{(+)}(pr),$$

with

$$\boxed{S_\ell(p) = \frac{B}{A}, \qquad \delta_\ell(p) = \frac{1}{2}\arg\left(\frac{B}{A}\right)}$$

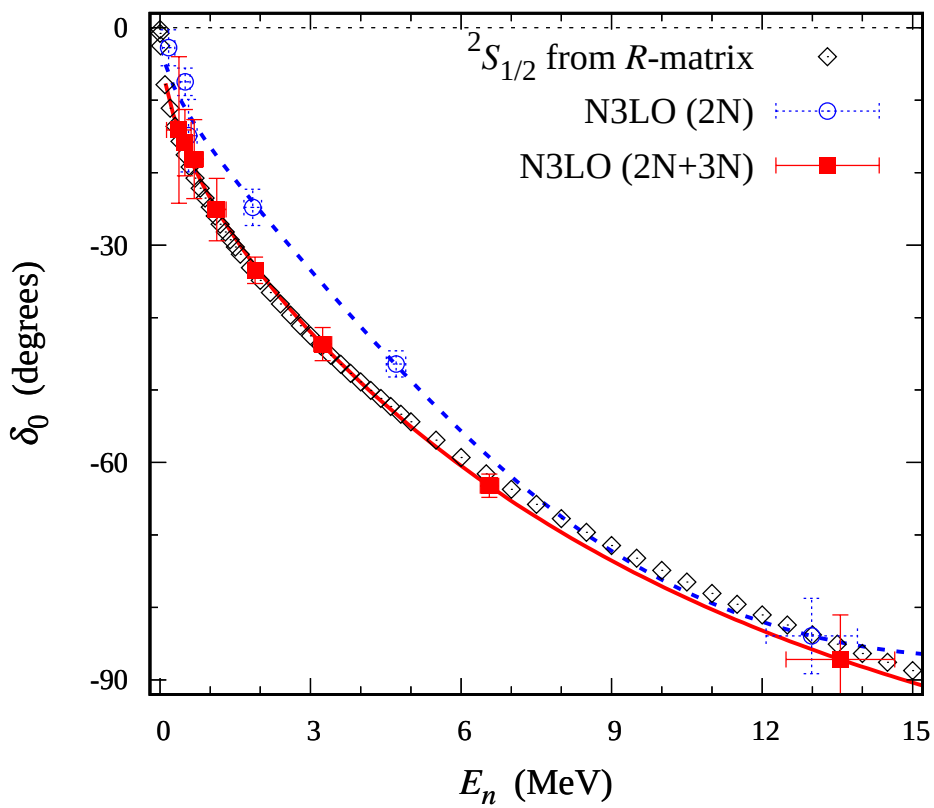
Therefore,

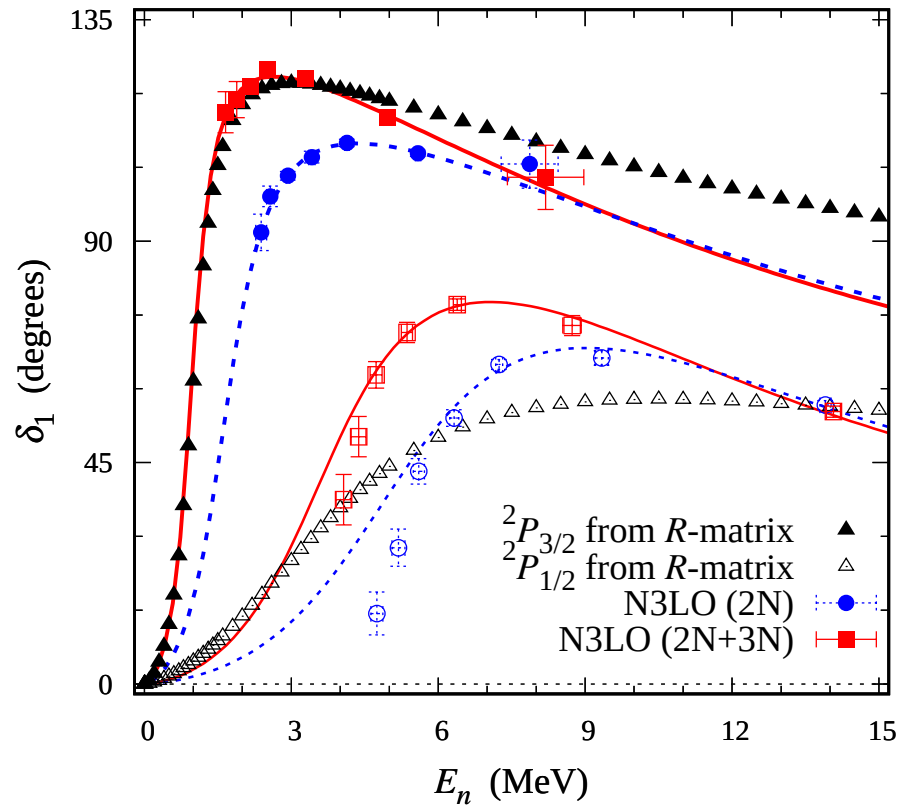
$$\boxed{\psi_\ell(r) \longrightarrow S_\ell(p) \longrightarrow \delta_\ell(p).}$$

The scattering information is extracted from **the radial wave function**.

Ab initio nuclear theory: neutron-alpha scattering at N3LO

$a = 1.32$ fm and $p_{\max} = \pi/a = 471$ MeV



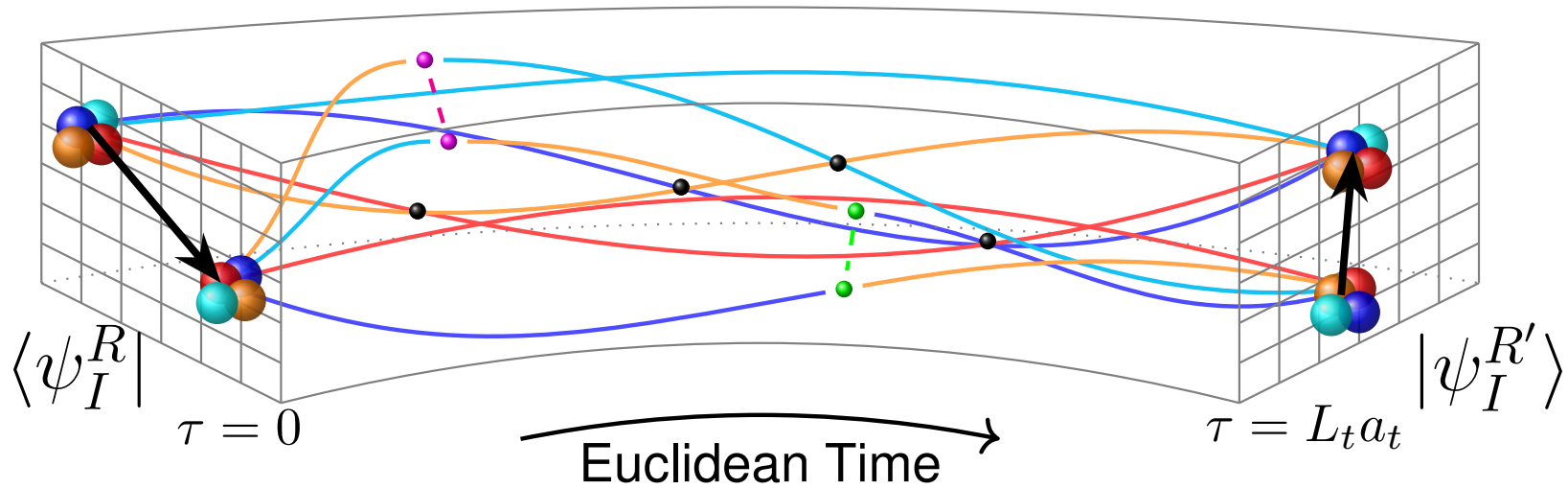


SE, Hildenbrand, Meißner J.Phys.G 52 (2025) 12, 125102

Scattering and reactions: Adiabatic projection method

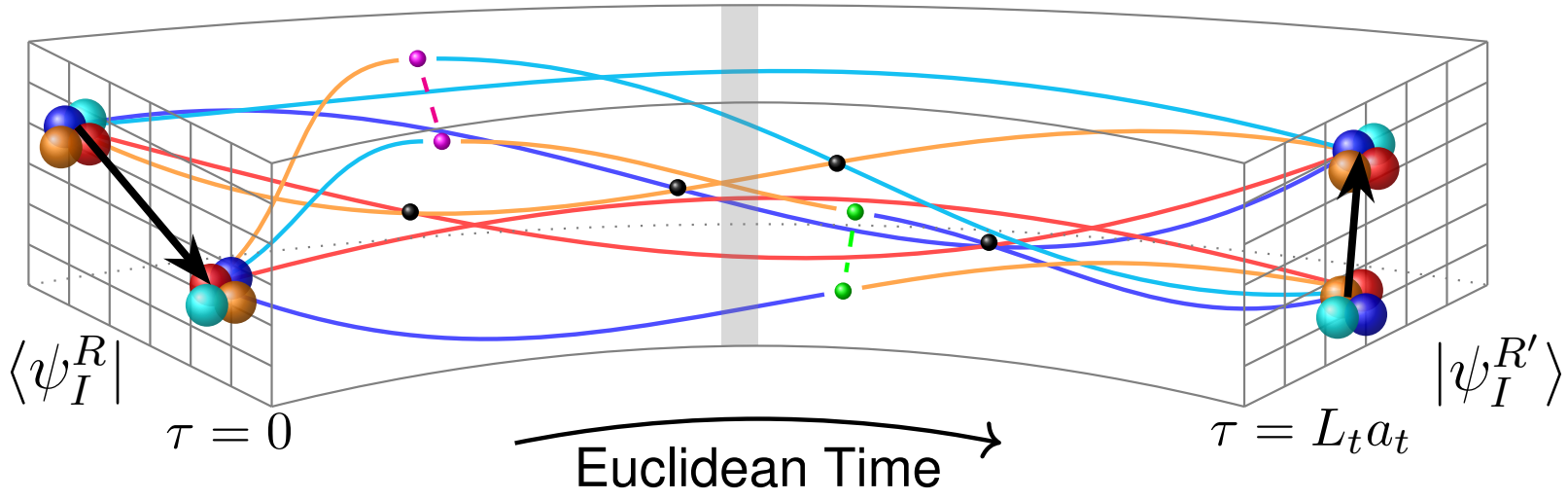
- The method constructs a low energy effective theory for the clusters.
- Use initial states parameterized by the relative spatial separation between clusters, and project them in Euclidean time.

$$|\psi_I^R\rangle = \sum_{\vec{r}} |\vec{r} + \vec{R}\rangle_1 \otimes |\vec{r}\rangle_2 \qquad \Longrightarrow \qquad |\psi_I^R\rangle_\tau = e^{-H\tau}\ |\psi_I^R\rangle$$



- The adiabatic projection in Euclidean time gives a systematically improvable description of the low- lying scattering cluster states.
- In the limit of large Euclidean projection time the description becomes exact.

Adiabatic projection method



Hamiltonian matrix

$$[H_\tau]^{J,J_z}_{R,R'} = {}^{J,J_z}_{\tau}\langle \psi_I^R | H | \psi_I^{R'} \rangle^{J,J_z}_{\tau}$$

Norm matrix

$$[N_\tau]^{J,J_z}_{R,R'} = {}^{J,J_z}_{\tau}\langle \psi_I^R | \psi_I^{R'} \rangle^{J,J_z}_{\tau}$$

$$[H^a_\tau]^{J,J_z}_{\vec{R},\vec{R}'} = \left[N_\tau^{-1/2} \; H_\tau \; N_\tau^{-1/2} \right]^{J,J_z}_{\vec{R}\,\vec{R}'}$$

Pine, Lee & Rupak *EPJA* 49 (2013) 151.

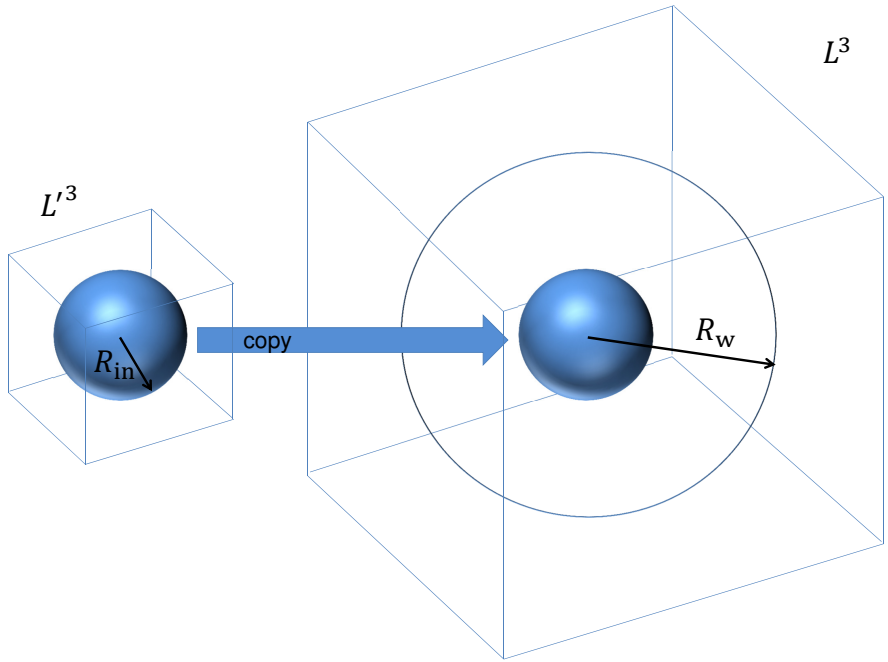
SE & Lee. *PRC* 90 064001 (2014).

SE, Lee, Rupak, Epelbaum, Krebs, Lähde, Luu, & Meißner. *Nature* 528, 111-114 (2015).

SE, Lee, Meißner & Rupak *EPJA* 52, 6, 174 (2016).

Adiabatic projection: separating dynamics from asymptotics

- **Interaction region:** compute the fully interacting $A_1 + A_2$ system only in a box slightly larger than the range of the inter-cluster interaction.
- **Asymptotic region:** propagate the two clusters in a much larger volume with the inter-cluster short-range interaction switched off (long-range Coulomb retained when present).
- Match the two descriptions at $R_{\rm in}$ and impose the spherical wall at R_w.

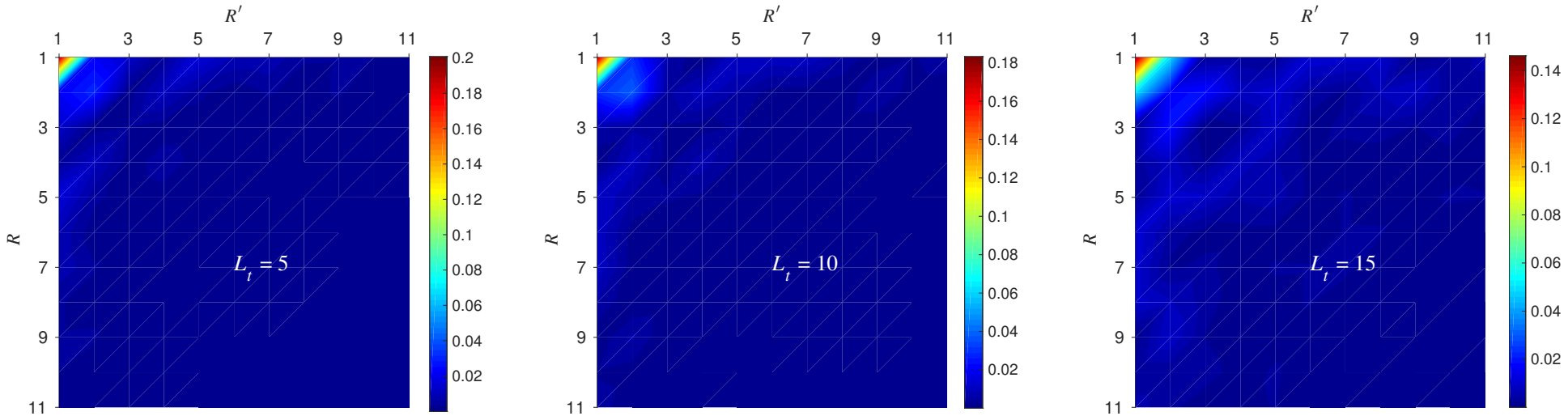


Large-volume energy resolution without a large-volume fully interacting many-body calculation.

SE, Lee, Meißner,Rupak. EPJA 52:174 (2016).

Asymptotic decoupling of the two-cluster dynamics

$$\Delta M_{L_t}(R, R') = \left| [M^a_{L_t}]_{R,R'} - [M_{\rm eff}]_{R,R'} \right| .$$



- The difference is concentrated in the region where the clusters overlap and interact.
- Away from this region, the interacting adiabatic transfer matrix approaches the effective two-cluster transfer matrix:

$$M^a_{L_t} \longrightarrow M_{\rm eff}.$$

- The short-distance many-body dynamics can be matched onto the large-volume asymptotic propagation with controlled finite-volume effects.

SE, Lee, Meißner,Rupak. EPJA 52:174 (2016).

Stabilizing the adiabatic Hamiltonian

$$H^a = N^{-1/2} H N^{-1/2}, \qquad N = O\,D\,O^\dagger, \qquad D = \mathrm{diag}(\lambda_1, \ldots, \lambda_M).$$

If the norm eigenvalues λ_α are small $\Rightarrow N^{-1/2}$ strongly amplifies poorly resolved Monte Carlo modes.

Tikhonov regularization

soft suppression

$$N_\kappa = N + \kappa A_n,$$

$$H^a(\kappa) = N_\kappa^{-1/2} H N_\kappa^{-1/2}.$$

- A_n projects onto the least-resolved norm eigenmodes.
- Lift only the small eigenvalues: suppress noise without modifying the well-resolved subspace.
- Calculate for several κ and extrapolate $\kappa \to 0$.

Norm-mode projection

hard suppression

$$\mathcal{K} = \{\alpha : \lambda_\alpha > \epsilon\lambda_1\},$$

$$X_\epsilon = O_\mathcal{K} D_\mathcal{K}^{-1/2} O_\mathcal{K}^\dagger, \qquad H_\epsilon^a = X_\epsilon H X_\epsilon.$$

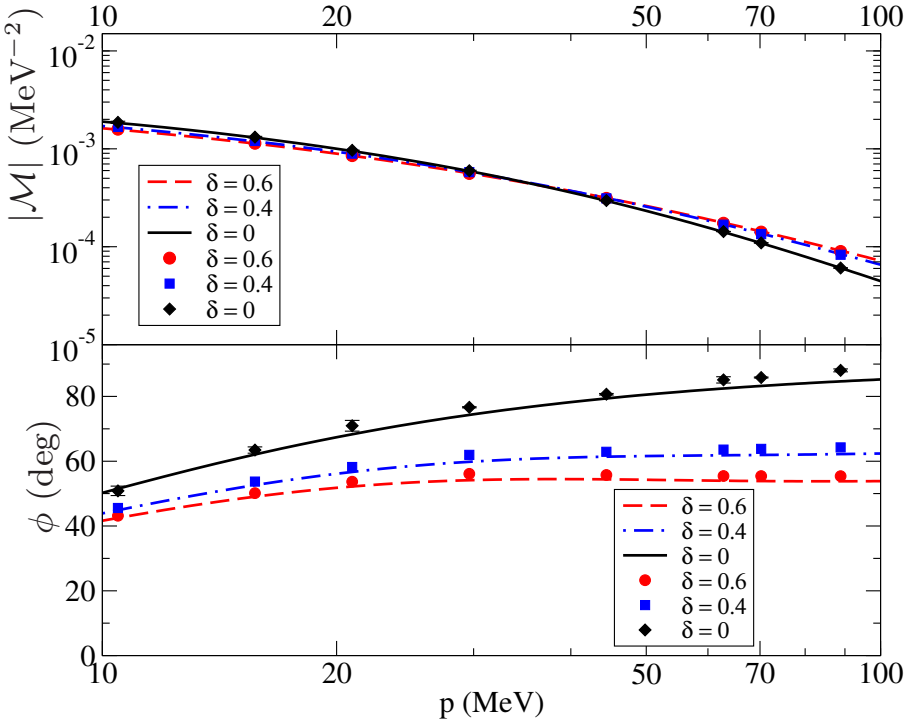
- Retain only the well-resolved eigenmodes of the norm matrix.
- Remove nearly-null *linear combinations* of radial states.
- No radial coordinate or radial bin itself is removed.

Sarkar, SE, Lähde & Meissner, arXiv:2606.28987

Meyer, SE, Hildenbrand & Meissner, arXiv:2607.00681

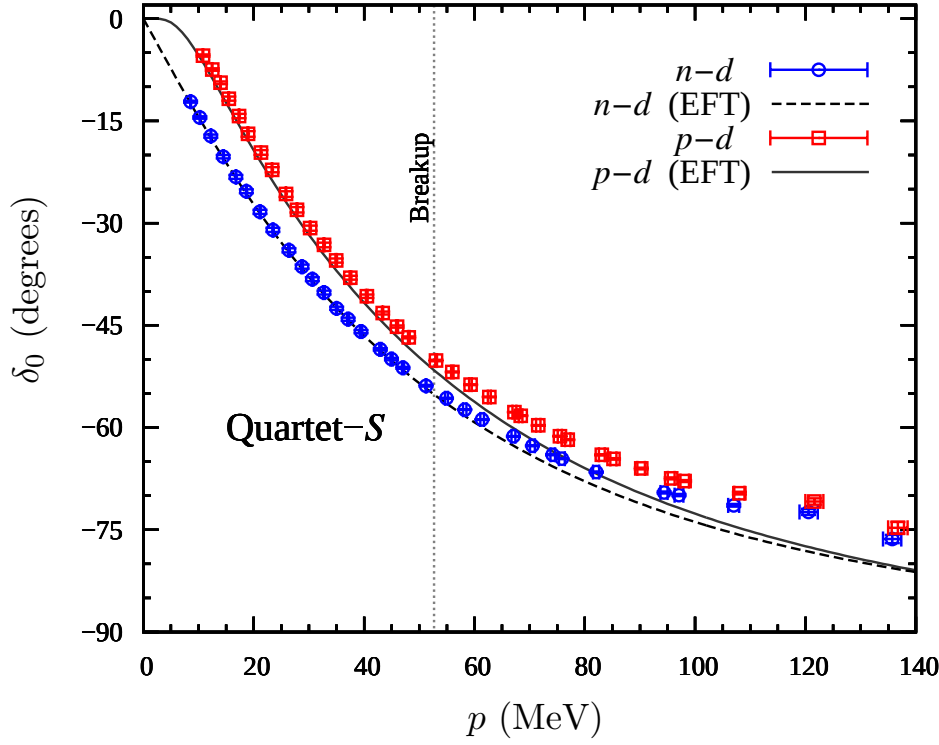
Ab *initio* nuclear scattering and reactions

The radiative capture process $p(n,\gamma)d$.



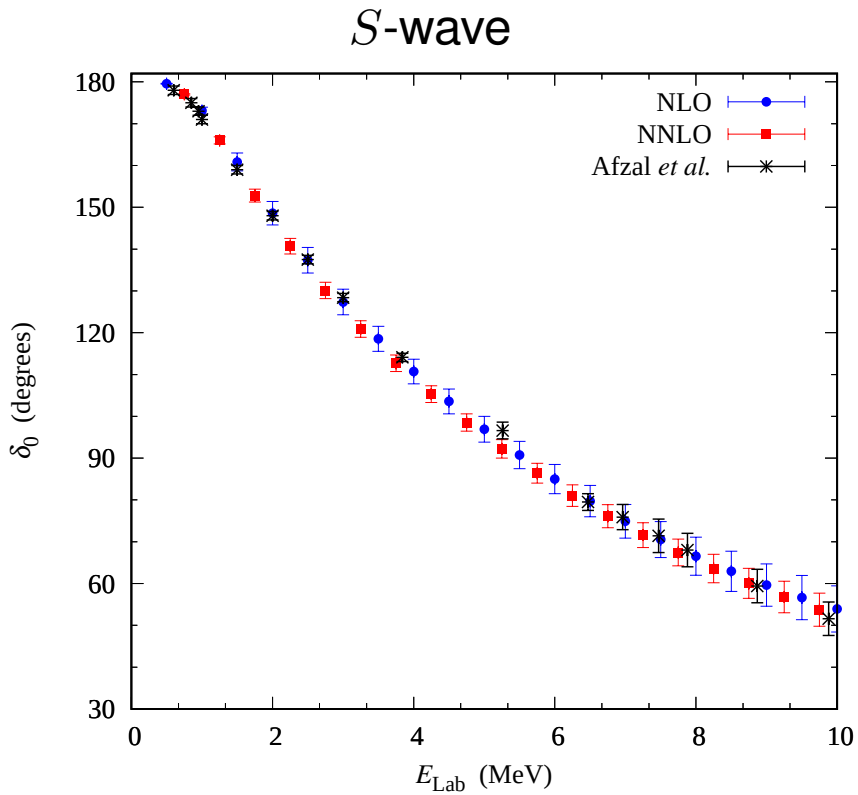
Rupak, Lee., PRL 111 (2013) 032502.

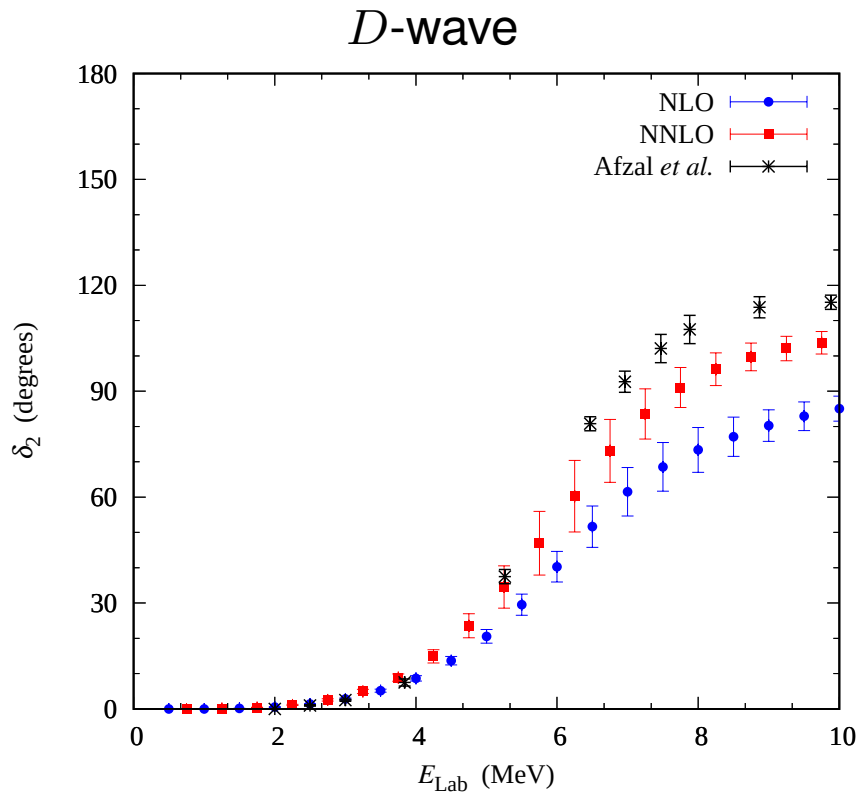
$N-d$ scattering.



SE, Lee, Meißner,Rupak. EPJA 52:174 (2016).

Ab initio nuclear scattering: alpha-alpha scattering





Afzal, Ahmad, Ali, Rev. Mod. Phys. 41, 247 (1969)

SE, Lee, Rupak, Epelbaum, Krebs, Lähde, Luu, Meißner, *Nature* 528, 111-114 (2015)

SE, Lähde, Lee, Meißner, Vonk *JHEP* 02, 001 (2022)

- Scattering and reaction processes involving alpha particle are in reach of ab initio methods
- This also has opened the door towards using experimental data from collisions of heavier nuclei as input to improve ab initio nuclear structure theory.

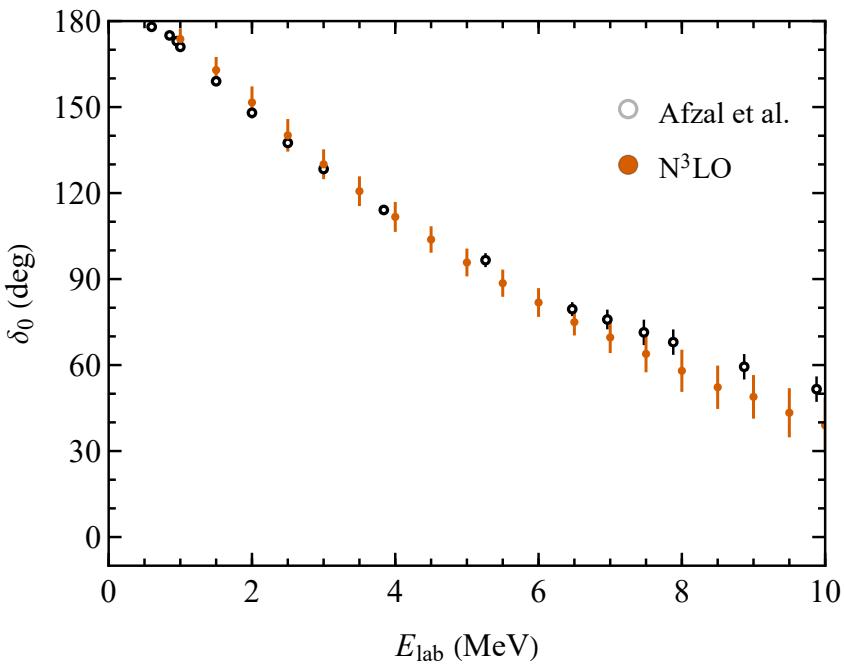
Ab initio nuclear scattering: alpha-alpha scattering at N3LO

- High-fidelity N^{3}LO interaction reproduces the empirical S- and D-wave systematics without scattering-specific refitting.
- The D wave resolves the broad 2^+ resonance of ^{8}Be:

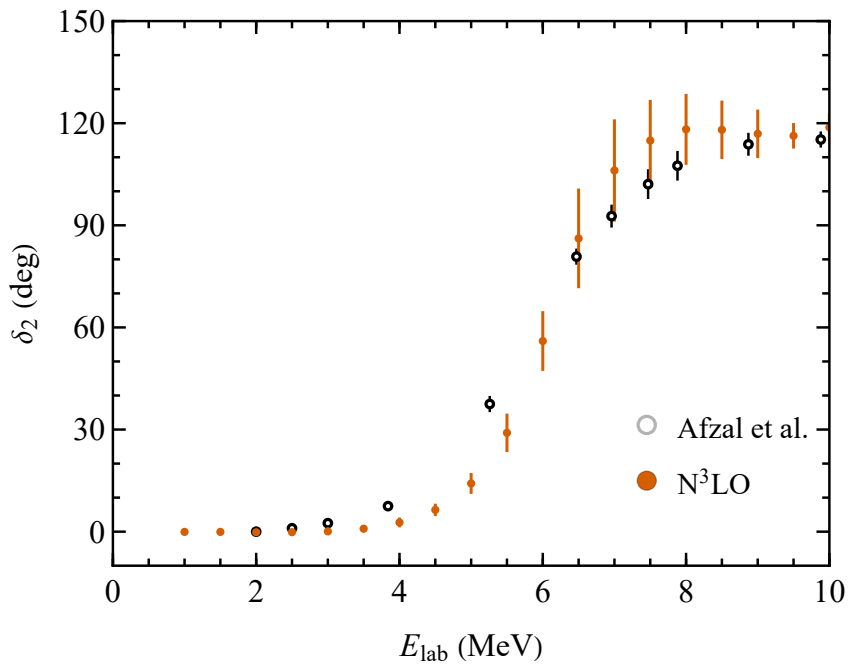
$$E_R = 3.25(25)\ \text{MeV}, \qquad \Gamma_R = 0.75(25)\ \text{MeV}.$$

- Remaining deviations provide new information on the short-range and three-nucleon interaction.

S-wave



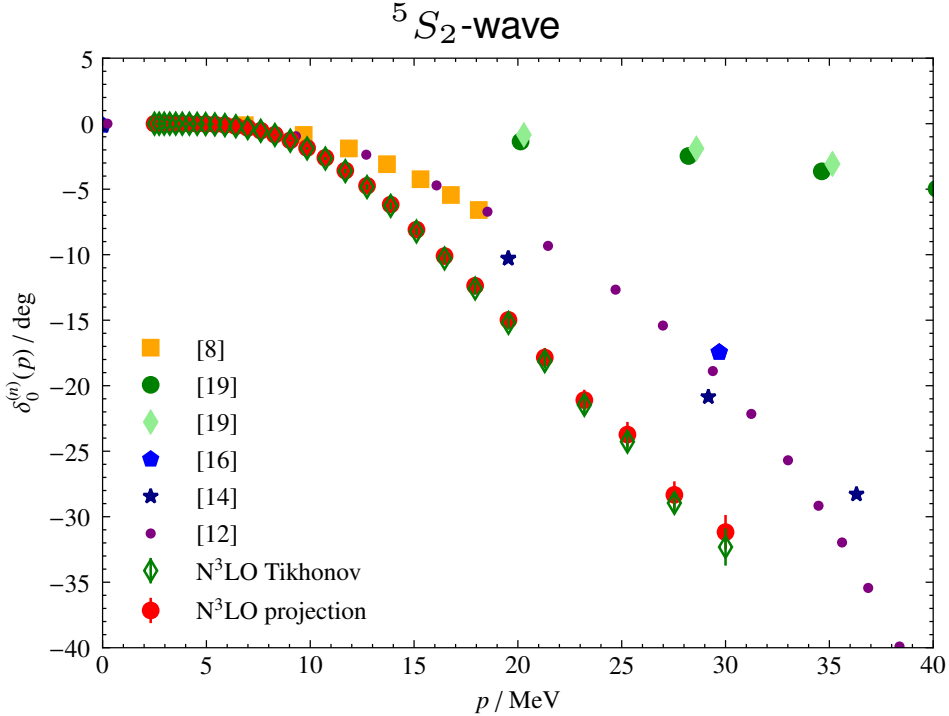
D-wave



Afzal, Ahmad, Ali, Rev. Mod. Phys. 41, 247 (1969)

Sarkar, SE, Lähde & Meissner, arXiv:2606.28987

Ab initio nuclear scattering: deutron-deutron scattering in the spin-quintet at N3LO



Meier, Glöckle, *Phys. A* 255 (1975) 21–34.
Carew, *Phys. Rev. C* 103 (1) (2021) 014002.
Hofmann, Hale, *Phys. Rev. C* 77 (2008) 044002.
Hofmann, Hale, *Phys. A* 613 (1997) 69–106.
Filikhin, Yakovlev, *Phys. Atom. Nucl.* 63 (2000).
Meyer, SE, Hildenbrand & Meissner, arXiv:2607.00681

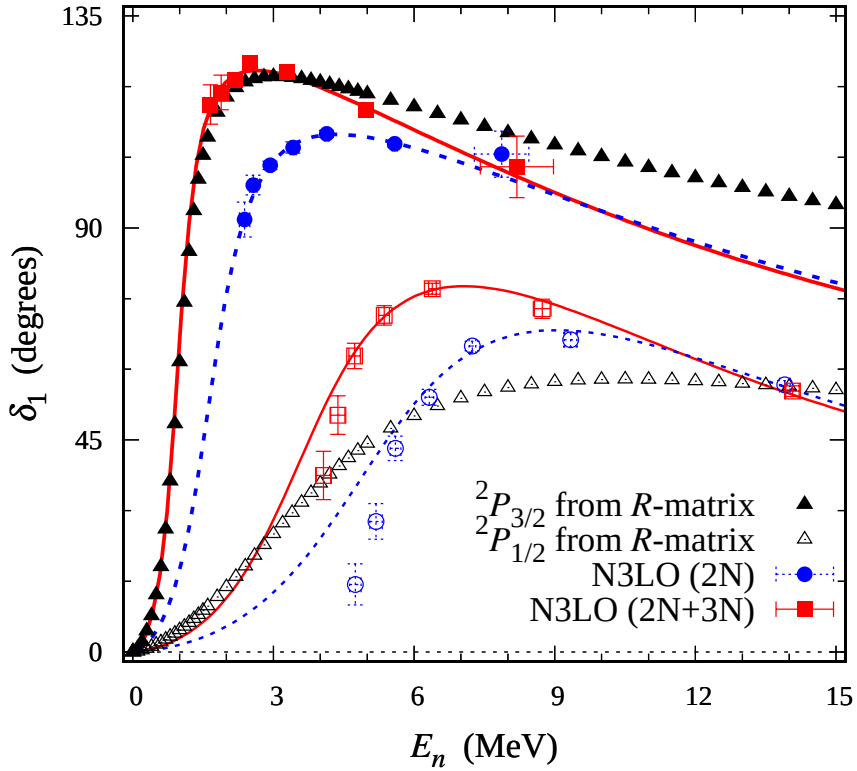
- Tikhonov regularization and norm-mode projection give consistent phase shifts.
- Coulomb-modified effective-range parameters:

$$^5a_{dd} = 12.96(26)\ \text{fm}, \qquad ^5r_{dd} = 3.62(79)\ \text{fm}.$$

- Present calculation: projected single $d + d\ ^5S_2$ asymptotic channel.

Next step: $\Longrightarrow$ $d + d \longleftrightarrow \begin{cases} n + {}^3\text{He}, \\ p + {}^3\text{H}. \end{cases}$

Ongoing: constraining the 3N interaction with $n - \alpha$ scattering



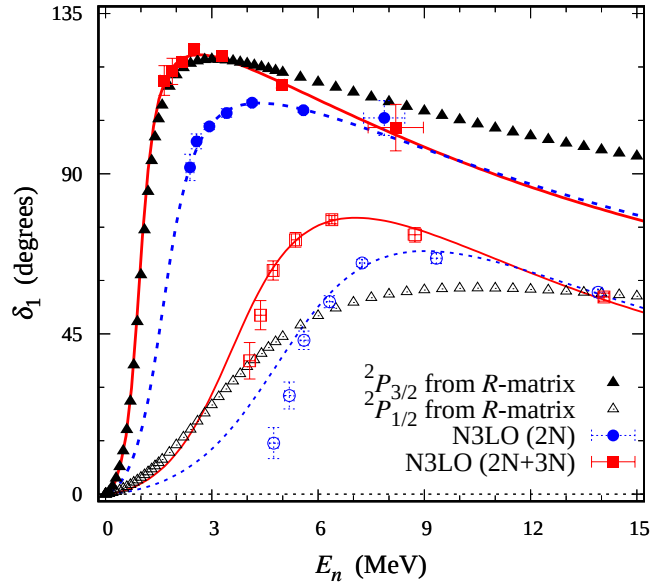
Partial-wave-resolved three-nucleon contact interactions: a pair of nucleons is projected onto a definite two-nucleon partial wave and the third nucleon couples to this pair through the scalar–isoscalar density $\rho^{(d)}(\vec{n})$.

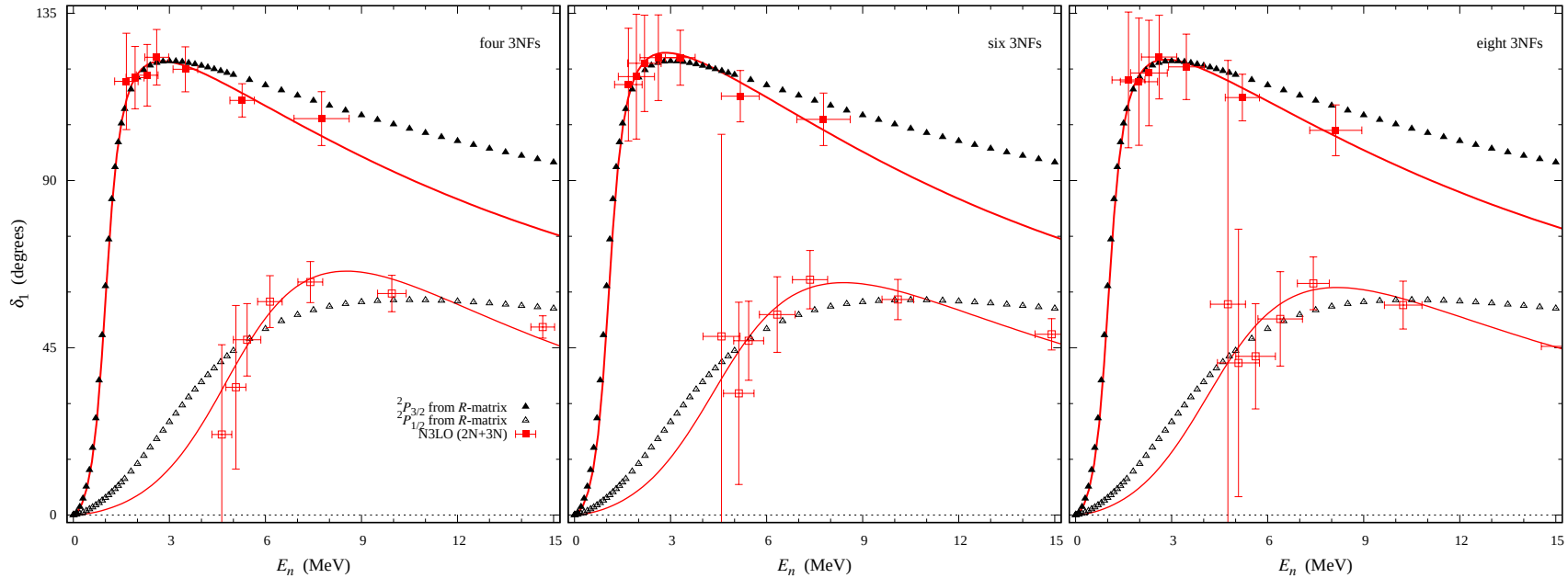
$$V^{(d)}_{3\mathrm{N},\alpha} = D^{(d)}_{\alpha} \sum_{\vec{n}} :\mathcal{O}^{\mathrm{PW}}_{\alpha}(\vec{n})\, \rho^{(d)}(\vec{n}):,$$

The pair operator is specified by $\alpha = \{I, S, J, L_i, L_f, n_i, n_f\}$.

Ongoing: constraining the 3N interaction with $n - \alpha$ scattering

Improved $2^P_{3/2}$ and $2^P_{1/2}$ splitting with recently used $V^{(d)}_{3\mathrm{N},\alpha}$ interactions on the lattice.





Summary and outlook

- **High-fidelity nuclear interactions on the lattice**
  Wavefunction matching makes realistic chiral interactions at N^{3}LO accessible to many-body lattice Monte Carlo calculations on a fine lattice.
- **The continuum provides a new and stringent test**
  n–α scattering demonstrates the sensitivity of P-wave resonances and spin-orbit splitting to the three-nucleon interaction.
- **Composite-cluster scattering is becoming quantitatively accessible**
  Adiabatic projection, finite-to-large-volume matching, and controlled norm-matrix regularization enable high-fidelity α–α and d–d calculations.
- **Recent results**
  N^{3}LO α–α scattering reproduces the empirical S- and D-wave systematics, while the first NLEFT d–d calculation establishes a benchmark for the ${}^5S_2$ channel.
- **Next step: from elastic scattering to reactions**
  Extend the same microscopic framework to coupled channels,

$$d + d \leftrightarrow \{\, n + {}^3\mathrm{He},\ p + {}^3\mathrm{H} \,\},$$

  neutron-induced reactions, and radiative capture.